

# The influence of the Mach number on the stability of radiative shocks

Babulakshmanan Ramachandran<sup>1\*</sup> & Michael D. Smith<sup>1,2†</sup>

<sup>1</sup>*Armagh Observatory, College Hill, Armagh BT61 9DG, Northern Ireland, U.K.*

<sup>2</sup>*Centre for Astrophysics & Planetary Science, The University of Kent, Canterbury, Kent CT2 7NR, U.K.*

Accepted ..... Received ..... ; in original form .....

## ABSTRACT

We study the stability properties of hydrodynamic shocks with finite Mach numbers. The linear analysis supplements previous analyses which took the strong shock limit. We derive the linearised equations for a general specific heat ratio as well as temperature and density power-law cooling functions, corresponding to a range of conditions relevant to interstellar atomic and molecular cooling processes. Boundary conditions corresponding to a return to the upstream temperature ( $R=1$ ) and to a cold wall ( $R=0$ ) are investigated. We find that for Mach number  $M > 5$ , the strong shock overstability limits are not significantly modified. For  $M < 3$ , however, shocks are considerably more stable for most cases. In general, as the shock weakens, the critical values of the temperature power-law index (below which shocks are overstable) are reduced for the overtones more than for the fundamental, which signifies a change in basic behaviour. In the  $R=0$  scenario, however, we find that the overstability regime and growth rate of the fundamental mode are increased when cooling is under local thermodynamic equilibrium. We provide a possible explanation for the results in terms of a stabilising influence provided downstream but a destabilising effect associated with the shock front. We conclude that the regime of overstability for interstellar atomic shocks is well represented by the strong shock limit unless the upstream gas is hot. Although molecular shocks can be overstable to overtones, the magnetic field provides a significant stabilising influence.

**Key words:** hydrodynamics – instabilities – shock waves – ISM: – ISM: molecules

## 1 INTRODUCTION

Across a shock front, a fraction of the bulk kinetic energy is thermalised. Across interstellar shock waves, the shock front is followed by a cooling layer in which a fraction of the thermal energy escapes as radiation. Across a *radiative* shock wave, the cooling time is much shorter than the dynamical evolution of the system. Such shocks propagate through many astrophysical media being driven by, for example, explosions, winds, jets and collisions (Shull & Draine 1987; Draine & McKee 1993). The fraction of energy which is thermalised in a steady-state hydrodynamic shock front can be simply expressed in terms of the specific heat ratio,  $\gamma$  and the Mach number,  $M$ , of the upstream (pre-shock) flow (Shull & Draine 1987). However, in some circumstances, radiative shocks are prone to an overstability due to the nature of the cooling (Chevalier & Imamura 1982, hereafter C182). In one-dimensional simulations, the oscillations of growing

amplitude can lead to a quasi-periodic collapse and restoration of almost the entire shock layer (e.g. Sutherland et al. 2003).

The overstability was first discovered by Langer et al. (1981). Soon after, Chevalier & Imamura (1982) performed a linear stability analysis for plane parallel flows with  $\Lambda \propto \rho^2 T^\alpha$ . They found that such shocks were linearly unstable in a fundamental mode if the exponent  $\alpha \lesssim 0.4$  and unstable to overtones for  $\alpha \lesssim 0.8$ . The physical basis for the instability is that, while the shock wave is moving away from the surface, it heats the gas to a higher temperature and the cooling time is longer than in the steady state case. As a result, in the unstable regime, the shock structure attempts to form an even larger cooling region. In contrast, while the shock wave is moving in, the situation is reversed thus yielding amplified oscillations.

A wide range of numerical and linear analyses have now catered for hot atomic gases in various physical and geometric forms (e.g. Imamura et al. 1984; Bertschinger 1986; Toth & Draine 1993; Dgani & Soker 1994; Imamura et al. 1996; Strickland & Blondin 1995; Sutherland et al. 2003).

\* E-mail: brc@arm.ac.uk

† E-mail: m.d.smith@kent.ac.uk

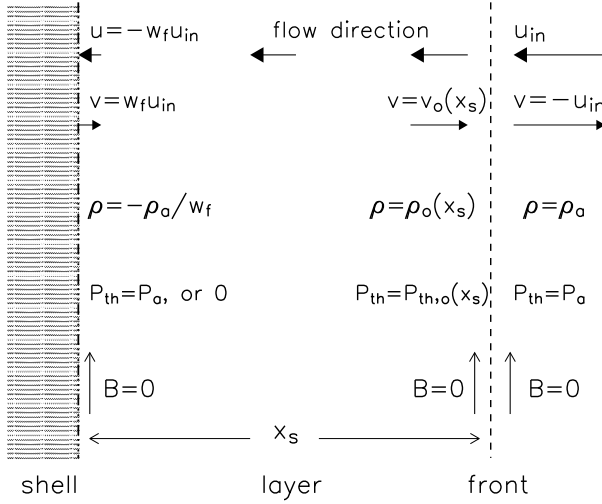


**Figure 1.** A sketch of the steady weak shock configuration. The shock jump conditions are defined by Eqs 4, 5 and 6. For weak shocks, we consider two cases: a final temperatures,  $T_a$ , corresponding to a shell of constant temperature equal to the upstream temperature or equal to zero, corresponding to accumulation onto a stationary wall.

Recently, Ramachandran & Smith (2005a, Paper I) provided a review while extending the linear analysis to show that the instability is not only sensitive to the cooling function but also to the specific heat ratio. Ramachandran & Smith (2005b, Paper II) analysed the corresponding magnetohydrodynamic case, thus considering both molecular and atomic shock waves. In fact, these linear analyses are only applicable to strong shocks in which the Mach number is assumed to be sufficiently large so that the shock profile is independent of the Mach number. Then, the front compression is  $(\gamma + 1)/(\gamma - 1)$  and the entire compression is effectively infinite unless limited by the magnetic field.

This leaves open the question of the dependence on the Mach number: for a given power-law cooling function, when is there a critical Mach number above which a shock is unstable? In fact, Strickland & Blondin (1995) performed numerical simulations taking  $\gamma = 5/3$  and found that low Mach number shocks were more stable than shocks with high Mach number. At lower  $M$ , it was found that the lower density in the cold gas layer acts like a shock absorber. In contrast, at high  $M$ , the layer is like a reflecting wall that rebounds incident waves. Although not comprehensive, a set of displayed simulations indicated that a shock unstable to overtone modes at high Mach number became stable for  $M$  somewhere in the range 5–10. Recently, Pittard et al. (2005) have also studied weak shocks numerically for a variety of boundary conditions and find that Mach numbers of order 100 are required before they are classified as strong shocks. They also find that the stability increases with the decrease in Mach number. Their study reveals that if the lower boundary condition is such that the post-shock gas cools to a temperature below the pre-shocked value, low

Mach number shocks reach critical values of  $\alpha$  which may be comparable to high Mach number shocks under the boundary condition in which the pre-shock and post-shock temperatures are the same.

To complement the above investigations as well as to extend the problem to molecular shocks, we have undertaken here a one-dimensional linear stability analysis with the Mach number as the main parameter while varying the specific heat ratio and two parameters,  $\alpha$  and  $\beta$ , which describe the cooling per unit volume in the form  $\Lambda \propto \rho^\beta T^\alpha$ . For evaluation, we pose a second question: for a given  $\beta$  and  $\gamma$ , how low must the Mach number be in order to significantly decrease the critical value of  $\alpha$  from the strong shock value?

## 2 METHOD

### 2.1 The steady state solution

The method employed here involves searching for wave modes which satisfy the equations representing linear perturbations away from the one-dimensional steady-state solution. We consider matter of constant density  $\rho_a$ , pressure  $P_a$ , temperature  $T_a$ , sound speed  $c_s$  and speed  $u_{in}$  which is incident on a stationary wall. As sketched in Fig. 1, the pre-shock gas velocity is  $v = -u_{in}$  where the shock speed  $u_{in}$  is defined as a positive quantity. Spatially, the origin  $x = 0$  is located at the wall or shock-shell interface, with the shock front lying at some distance  $x = x_s$ . In the case where the final temperature returns to the upstream value, the post-shock gas passes through the cooling region and is added to the uniform density shell. In the case where the final temperature is zero, the matter is added to an infinitely thin region at the rigid wall. In both cases, the length  $x_s$  is the thickness of the cooling region.

The one dimensional hydrodynamical equations are

$$\frac{\partial \rho}{\partial t} + \rho \frac{\partial v}{\partial x} + v \frac{\partial \rho}{\partial x} = 0, \quad (1)$$

$$\rho \left( \frac{\partial v}{\partial t} + v \frac{\partial v}{\partial x} \right) + \frac{\partial P}{\partial x} = 0, \quad (2)$$

$$\frac{\partial P}{\partial t} + v \frac{\partial P}{\partial x} - \frac{\gamma P}{\rho} \left( \frac{\partial \rho}{\partial t} + v \frac{\partial \rho}{\partial x} \right) = -(\gamma - 1) A \rho^{\beta - \alpha} P^\alpha, \quad (3)$$

where equations (1), (2) & (3) refer to the conservation of mass, momentum and energy, respectively. In equation (3),  $A$  is a constant. The steady state solution is denoted by the subscript 0.

The Rankine-Hugoniot conditions provide the values of the physical variables at  $x = x_s$ . These are

$$\rho_0(x_s) = \left[ \frac{(\gamma + 1) M^2}{(\gamma - 1) M^2 + 2} \right] \rho_a, \quad (4)$$

$$v_0(x_s) = - \left[ \frac{(\gamma - 1) M^2 + 2}{(\gamma + 1) M^2} \right] u_{in}, \quad (5)$$

$$P_0(x_s) = \left[ \frac{2\gamma M^2 - (\gamma - 1)}{\gamma(\gamma + 1) M^2} \right] \rho_a u_{in}^2. \quad (6)$$

where  $M = \frac{u_{in}}{c_s}$  is the Mach number and  $c_s$  is the sound speed (e.g. Priest 1982; Shore 1993). Equations (4), (5) &

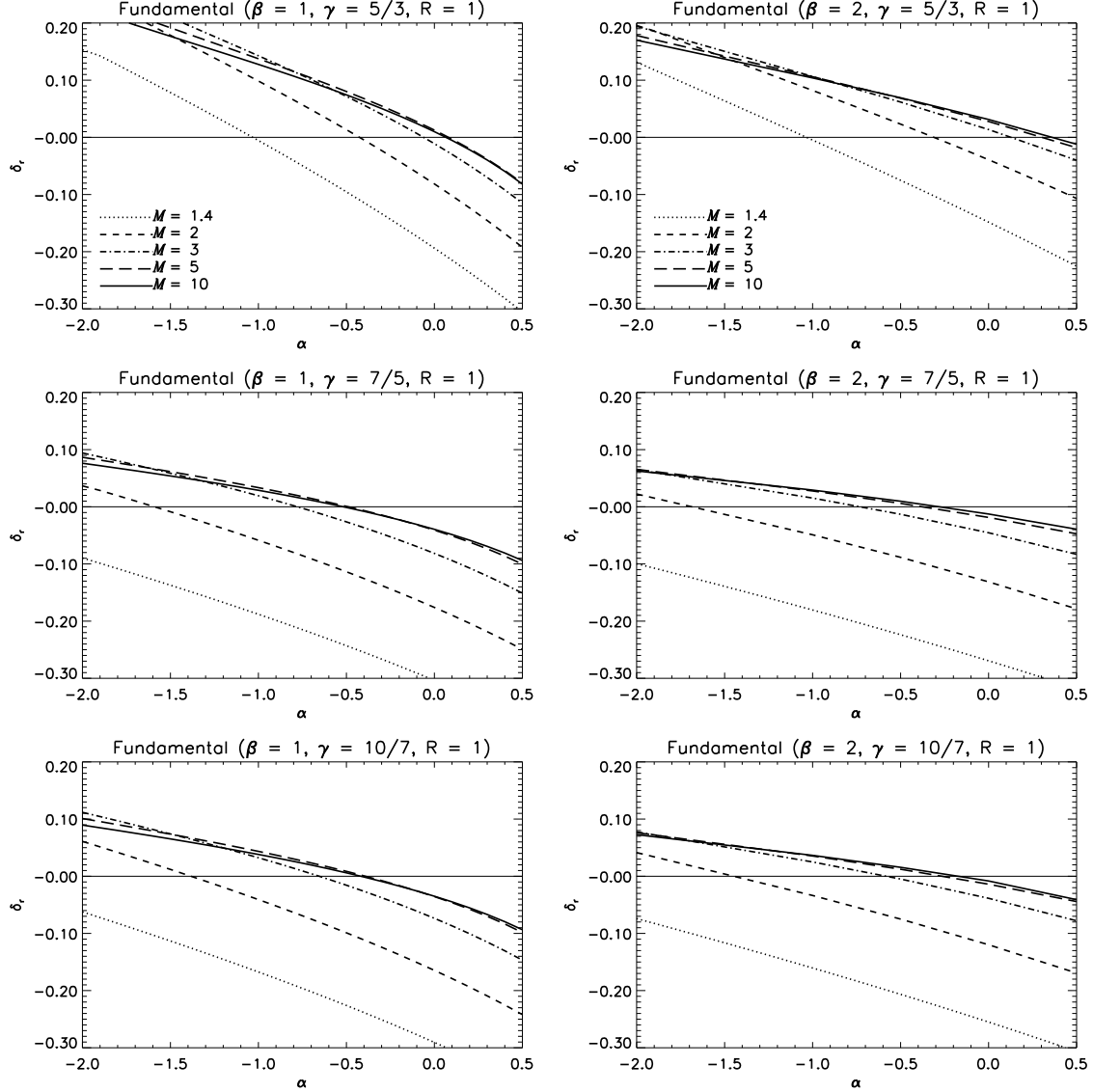


**Figure 2.** The growth/damping rates,  $\delta_r$ , as a function of  $\alpha$  for the fundamental mode with  $R=1$ . Values of  $\gamma$ ,  $\beta$  and  $M$  are indicated.

(6) are obtained when equations (1) and (2) are integrated to yield

$$\rho_0 v_0 = -\rho_a u_{in}, \quad (7)$$

$$P_0 = \rho_a u_{in}(v_0 + u_{in}) + P_a. \quad (8)$$

Equations (7) & (8) are substituted in equation (3) to obtain

$$\frac{dv_0}{dx} = \frac{-(\gamma-1)A(\rho_a u_{in})^{\beta-1} \left[ -v_0^2 - u_{in} v_0 \left( 1 + \frac{1}{\gamma M^2} \right) \right]^\alpha}{(-v_0)^\beta \left[ v_0 + \gamma \left( v_0 + u_{in} \left( 1 + \frac{1}{\gamma M^2} \right) \right) \right]}. \quad (9)$$

We now introduce the following variables

$$\xi = \frac{x}{x_s}, \quad (10)$$

$$w = \frac{v_0}{u_{in}}. \quad (11)$$

Equations (9), (10) and (11) lead to

$$\frac{d\xi}{dw} = \frac{-(-w)^\beta u_{in}^{3-2\alpha} \left[ w + \gamma \left( w + 1 + \frac{1}{\gamma M^2} \right) \right]}{(\gamma-1)A\rho_a^{\beta-1} x_s \left[ -w \left( w + 1 + \frac{1}{\gamma M^2} \right) \right]^\alpha}. \quad (12)$$

## 2.2 The steady state boundary conditions

Before we can integrate equation (12), we must specify the boundary conditions. We consider two scenarios. The first case is when the temperature at the shell is the same as the temperature of the pre-shock medium and the second case is when the temperature drops to zero. Therefore, we define a quantity  $R$  as the ratio of the temperature at the shell to that of the pre-shock temperature. If  $R = 1$ , then we have the former case and if  $R = 0$ , we have the latter.

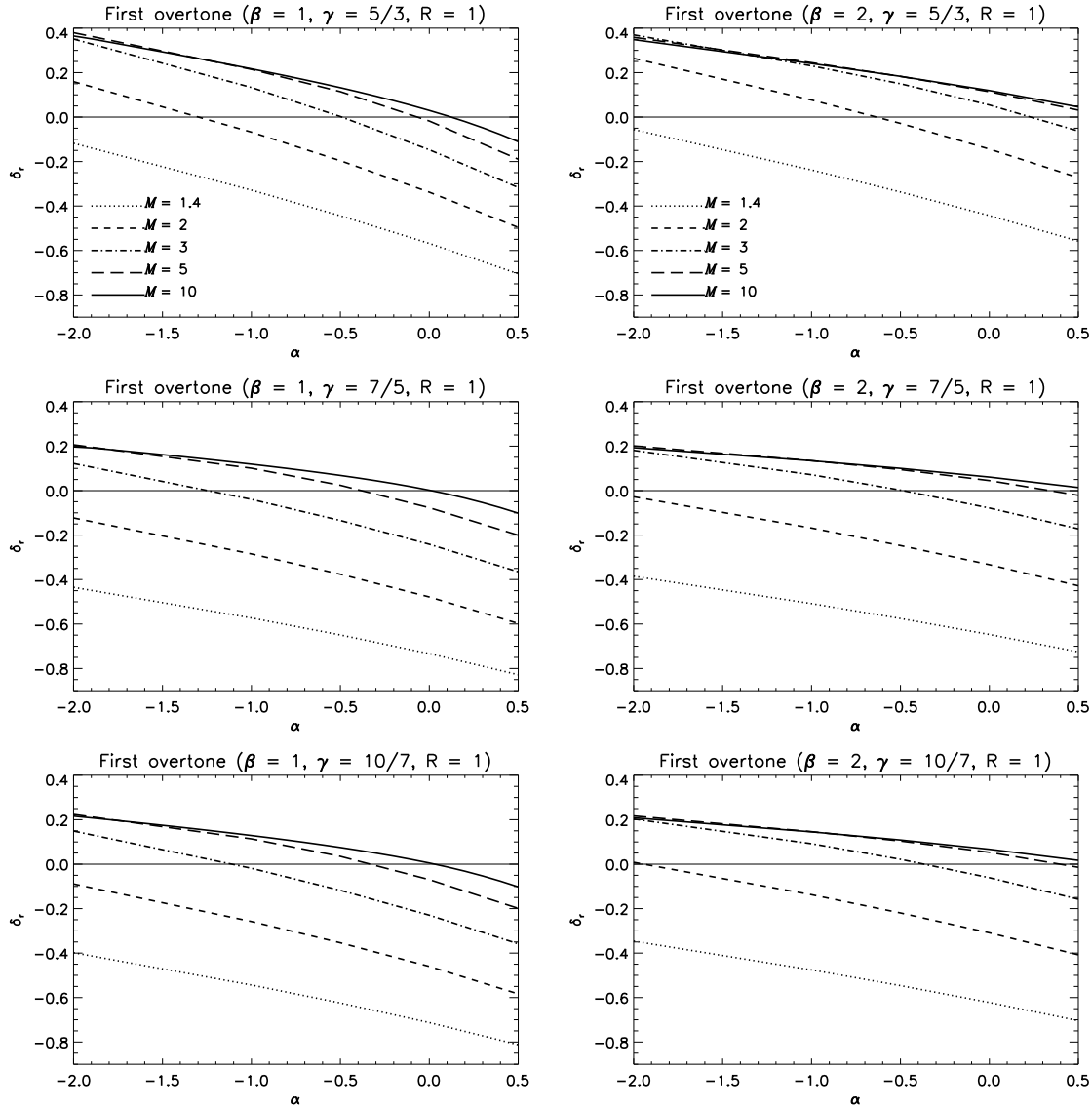


**Figure 3.** The growth/damping rates,  $\delta_r$ , as a function of  $\alpha$  for the first overtone mode with  $R = 1$ . Values of  $\gamma$ ,  $\beta$  and  $M$  are indicated.

$$R = \frac{\left(\frac{P_0}{\rho_0}\right)}{\left(\frac{P_a}{\rho_a}\right)}. \quad (13)$$

This results in

$$w^2 + w \left[ 1 + \frac{1}{\gamma M^2} \right] + \frac{R}{\gamma M^2} = 0 \quad (14)$$

We consider only the roots that are physical and hence the boundary conditions are

$$w = 0 \quad \text{at} \quad \xi = 0 \quad (R = 0) \quad (15)$$

$$w = -\left(\frac{1}{\gamma M^2}\right) \quad \text{at} \quad \xi = 0 \quad (R = 1) \quad (16)$$

$$w = -\left[\frac{(\gamma - 1)M^2 + 2}{(\gamma + 1)M^2}\right] \quad \text{at} \quad \xi = 1. \quad (17)$$

The shock width  $x_s$  is evaluated in the process.

### 3 THE SET OF LINEAR EQUATIONS

The shock wave is now perturbed by

$$\frac{dx_s}{dt} = v_{s1} e^{\sigma t}, \quad (18)$$

where  $\sigma = \sigma_R + i\sigma_I$  is the frequency and  $v_{s1}$  is a real quantity. The position of the shock may be represented as the real part of

$$x_s = x_{s0} + x_{s1} e^{\sigma t}, \quad (19)$$

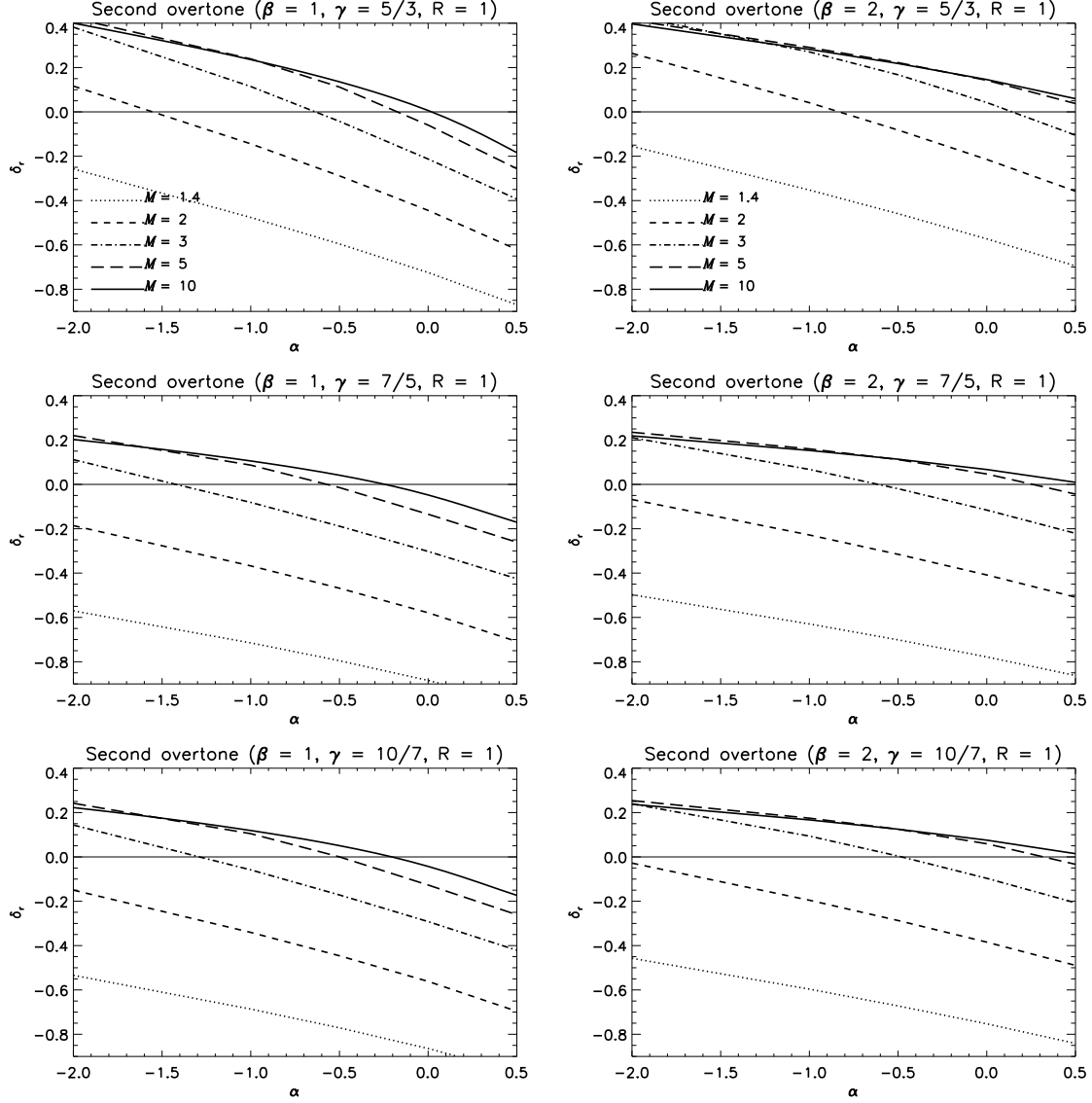


**Figure 4.** The growth/damping rates,  $\delta_r$ , as a function of  $\alpha$  for the second overtone with  $R=1$ . Values of  $\gamma$ ,  $\beta$  and  $M$  are indicated.

where  $x_{s1} = \frac{v_{s1}}{\sigma}$ . Considering only the terms up to first order:

$$\xi = \frac{x}{x_s} = \frac{x}{x_{s0}} \left( 1 - \frac{x_{s1}}{x_{s0}} e^{\sigma t} \right), \quad (20)$$

$$\frac{\partial \xi}{\partial x} = \frac{1}{x_{s0}} \left( 1 - \frac{x_{s1}}{x_{s0}} e^{\sigma t} \right), \quad (21)$$

$$\frac{\partial \xi}{\partial t} = -\frac{x x_{s1} \sigma e^{\sigma t}}{x_{s0}^2}, \quad (22)$$

$$\rho = \rho_0(\xi) + \rho_1(\xi) e^{\sigma t}, \quad (23)$$

$$P = P_0(\xi) + P_1(\xi) e^{\sigma t}, \quad (24)$$

$$v = v_0(\xi) + v_1(\xi) e^{\sigma t}. \quad (25)$$

All the quantities with subscript 1 represent the small perturbed factors. The boundary conditions at the shock wave

are (see Appendix A)

$$\rho_1 = \left[ \frac{4v_{s1}\rho_a(\gamma+1)M^2}{u_{in}[2+(\gamma-1)M^2]^2} \right], \quad (26)$$

$$P_1 = \left( \frac{4u_{in}v_{s1}\rho_a}{\gamma+1} \right), \quad (27)$$

$$v_1 = \frac{2v_{s1}}{\gamma+1} \left[ 1 + \frac{1}{M^2} \right]. \quad (28)$$

We then transform the following variables as

$$\zeta = \frac{x_{s0}\sigma\rho_1}{v_{s1}\rho_a} \quad (29)$$

$$\pi = \frac{P_1}{v_{s1}\rho_a u_{in}} \quad (30)$$

$$\eta = \frac{v_1}{v_{s1}} \quad (31)$$

$$\delta = \frac{x_{s0}\sigma}{u_{in}}. \quad (32)$$

Substituting (23), (24), (25) into (1), (2) and (3), the fluid

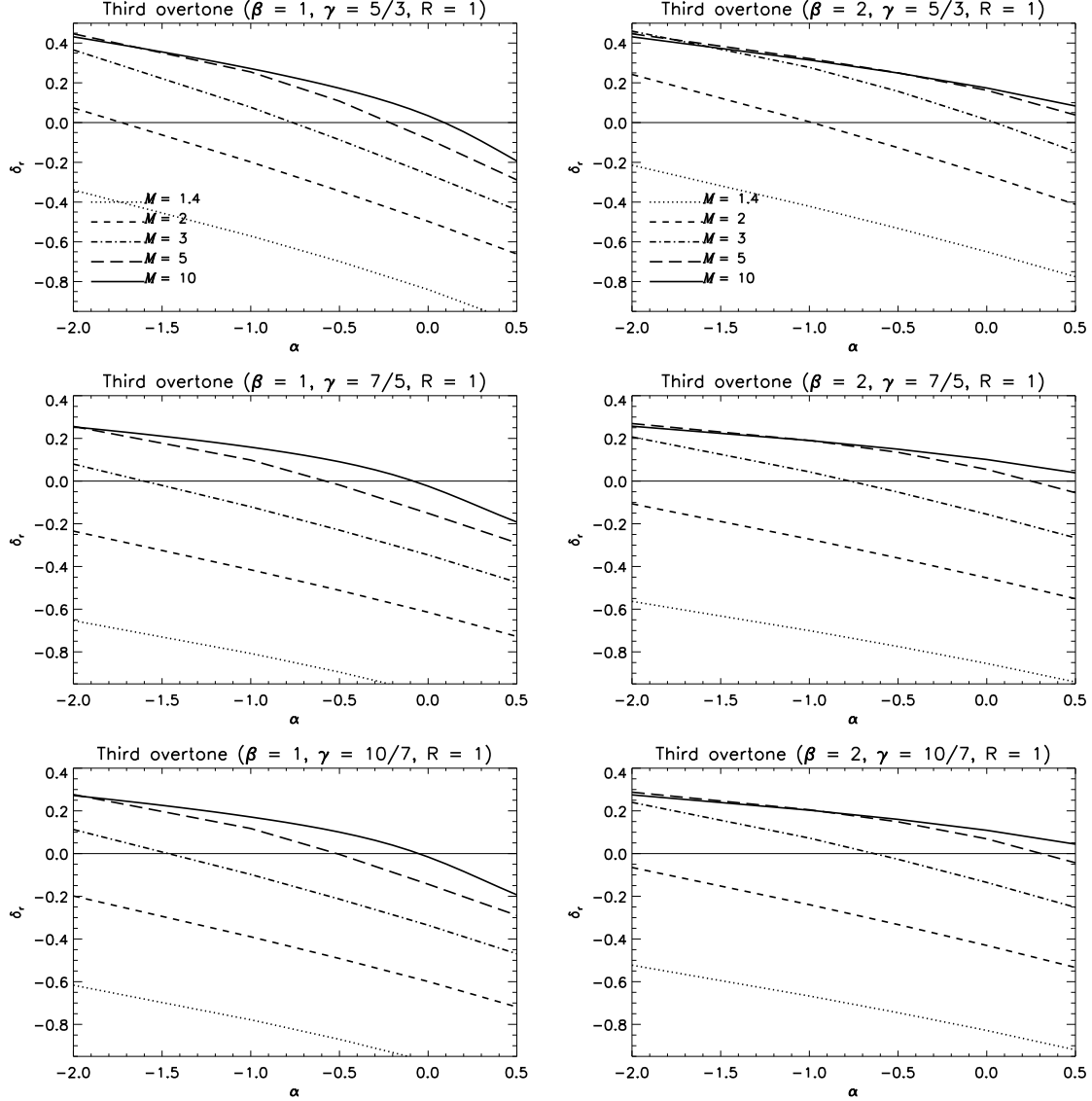


**Figure 5.** The growth/damping rates,  $\delta_r$ , as a function of  $\alpha$  for the third overtone with  $R=1$ . Values of  $\gamma$ ,  $\beta$  and  $M$  are indicated.

equations become

$$-\frac{\xi}{w^2} + \zeta \frac{d\xi}{dw} + \frac{w}{\delta} \frac{d\zeta}{dw} + \frac{\eta}{w^2} - \frac{1}{w} \frac{d\eta}{dw} + \frac{\zeta}{\delta} = 0 \quad (33)$$

$$-\xi + \delta \frac{d\xi}{dw} \eta + w \frac{d\eta}{dw} + \eta - \frac{w^2}{\delta} \zeta - w \frac{d\pi}{dw} = 0 \quad (34)$$

$$D + E = F \quad (35)$$

where

$$\begin{aligned} D &= \left[ -\xi + \delta \frac{d\xi}{dw} \pi + w \frac{d\pi}{dw} + \eta - \frac{w}{\delta} + \pi \gamma \right] \\ E &= \left( -\frac{\xi}{w^2} + \zeta \frac{d\xi}{dw} + \frac{w}{\delta} \frac{d\zeta}{dw} + \frac{\eta}{w^2} - \frac{1}{\delta w} + \frac{\zeta}{\delta} \right) \\ &\quad \times \left[ \gamma w \left( w + 1 + \frac{1}{\gamma M^2} \right) \right] \\ F &= \left[ w + \gamma \left( 1 + w + \frac{1}{\gamma M^2} \right) \right] \\ &\quad \times \left[ \frac{\alpha \pi}{\left( 1 + w + \frac{1}{\gamma M^2} \right)} - (\beta - \alpha) \frac{w \zeta}{\delta} \right] \end{aligned} \quad (36)$$

The quantities  $\zeta$ ,  $\pi$  and  $\eta$  are complex eigenfunctions where the subscript  $r$  denotes the real component and  $i$  stands for the imaginary part for each of the above quantities. The quantity  $\delta$  is a complex number with the sign of the real part,  $\delta_r$  indicating the instability (+ve value) or stability

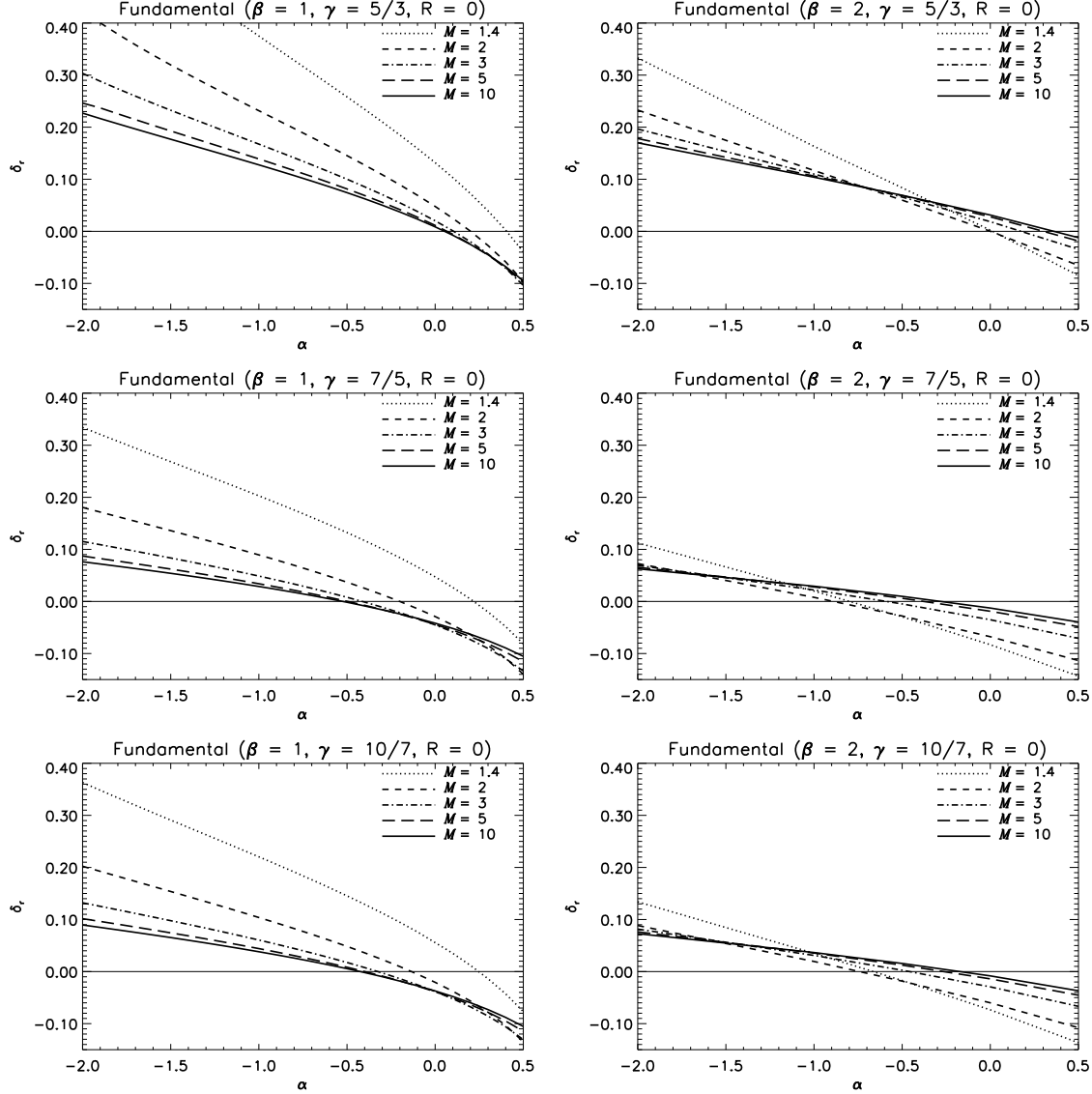


**Figure 6.** The growth/damping rates,  $\delta_r$ , as a function of  $\alpha$  for the fundamental mode with  $R=0$ . Values of  $\gamma$ ,  $\beta$  and  $M$  are indicated.

(-ve value) of a mode. The quantity  $\delta_i$  is interpreted as the eigenfrequency (in units of  $(u_{in}/x_{s0})$ ).

and (35), we get six coupled first order equations which are

$$\begin{aligned} \frac{d\eta_r}{dw} = & \frac{\alpha\pi_r}{\left(w + 1 + \frac{1}{\gamma M^2}\right)} - \frac{w(\beta - \alpha)(\delta_r\zeta_r + \delta_i\zeta_i)}{\delta^2} + \frac{\delta_r}{\delta^2} \\ & + \frac{2\xi\delta^2 - 2\eta_r\delta^2 - \gamma\pi_r\delta^2 + w^2(\zeta_r\delta_r + \zeta_i\delta_i)}{\left[w + \gamma\left(w + 1 + \frac{1}{\gamma M^2}\right)\right]\delta^2} \\ & - \frac{d\xi}{dw} \left[ \frac{\delta_r(\eta_r + \pi_r) - \delta_i(\eta_i + \pi_i)}{\left(w + \gamma\left(w + 1 + \frac{1}{\gamma M^2}\right)\right)} \right] \end{aligned} \quad (37)$$

$$\begin{aligned} \frac{d\eta_i}{dw} = & \frac{\alpha\pi_i}{\left(w + 1 + \frac{1}{\gamma M^2}\right)} - \frac{w(\beta - \alpha)(\delta_r\zeta_i - \delta_i\zeta_r)}{\delta^2} - \frac{\delta_i}{\delta^2} \\ & + \frac{-2\eta_i\delta^2 - \gamma\pi_i\delta^2 + w^2(\zeta_i\delta_r - \zeta_r\delta_i)}{\left[w + \gamma\left(w + 1 + \frac{1}{\gamma M^2}\right)\right]\delta^2} \\ & - \frac{d\xi}{dw} \left[ \frac{\delta_i(\eta_r + \pi_r) + \delta_r(\eta_i + \pi_i)}{\left(w + \gamma\left(w + 1 + \frac{1}{\gamma M^2}\right)\right)} \right] \end{aligned} \quad (38)$$

Substituting Eqs. (30), (31) and (32) in Eqns. (33), (34)

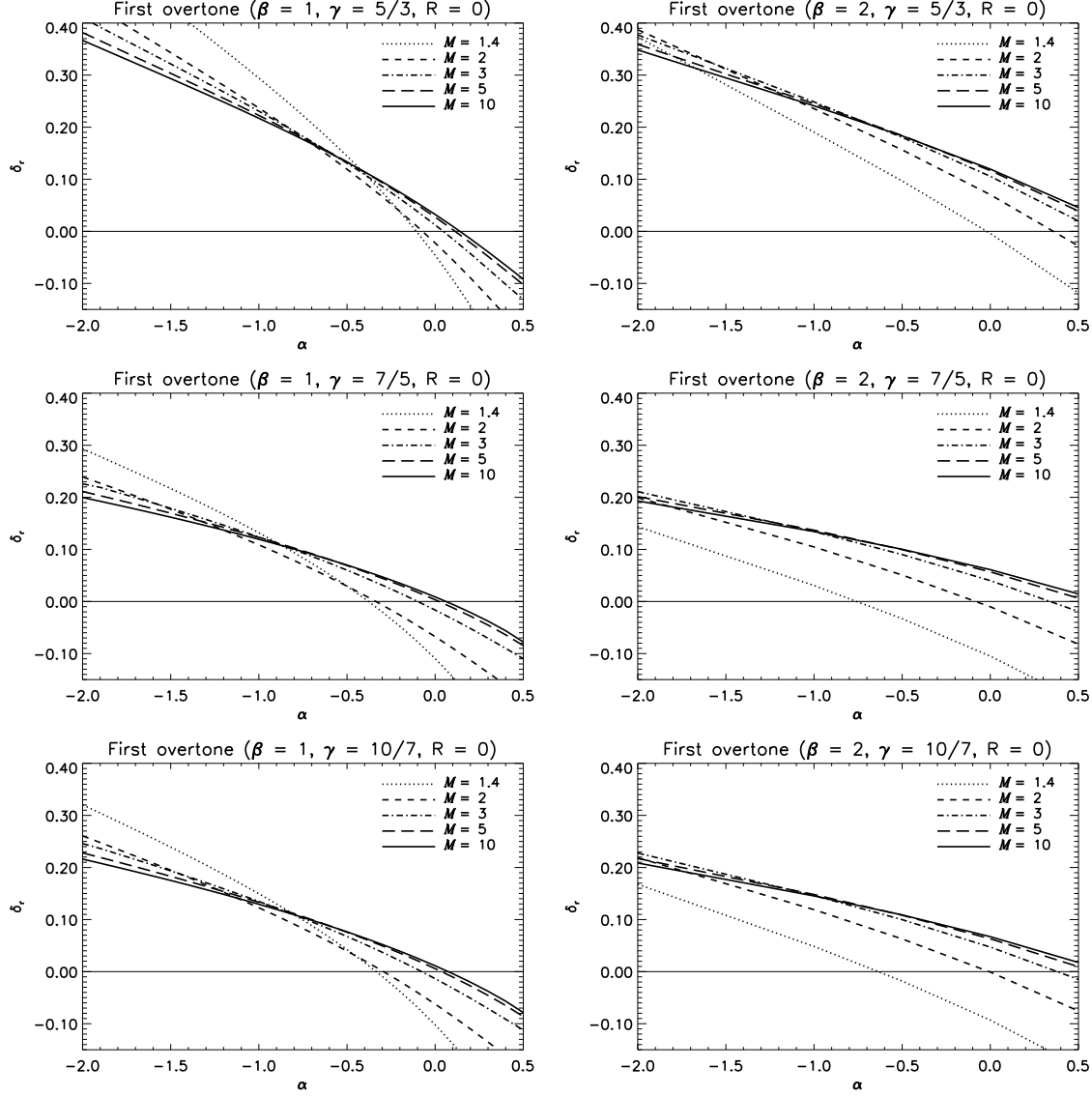


**Figure 7.** The growth/damping rates,  $\delta_r$ , as a function of  $\alpha$  for the first overtone mode with  $R=0$ . Values of  $\gamma$ ,  $\beta$  and  $M$  are indicated.

$$\frac{d\pi_r}{dw} = \frac{-\xi}{w} + \frac{(\delta_r\eta_r - \delta_i\eta_i)}{w} \frac{d\xi}{dw} + \frac{\eta_r}{w} + \frac{d\eta_r}{dw} - \frac{w(\zeta_r\delta_r + \zeta_i\delta_i)}{\delta^2} \quad (39)$$

$$\begin{aligned} \frac{d\zeta_r}{dw} &= \frac{\xi\delta_r}{w^3} - \frac{d\xi}{dw} \frac{\zeta_r\delta_r}{w} + \frac{\delta_r}{w^2} \frac{d\eta_r}{dw} - \frac{\eta_r\delta_r}{w^3} \\ &\quad - \frac{\delta_r(\zeta_r\delta_r + \zeta_i\delta_i)}{w\delta^2} + \frac{d\xi}{dw} \frac{\zeta_i\delta_i}{w} - \frac{\delta_i}{w^2} \frac{d\eta_i}{dw} \\ &\quad + \frac{\eta_i\delta_i}{w^3} + \frac{\delta_i(\zeta_i\delta_r - \zeta_r\delta_i)}{w\delta^2} \end{aligned} \quad (41)$$

$$\begin{aligned} \frac{d\zeta_i}{dw} &= \frac{\xi\delta_i}{w^3} - \frac{d\xi}{dw} \frac{\zeta_i\delta_r}{w} + \frac{\delta_r}{w^2} \frac{d\eta_i}{dw} - \frac{\eta_i\delta_r}{w^3} \\ &\quad - \frac{\delta_r(\zeta_i\delta_r - \zeta_r\delta_i)}{w\delta^2} - \frac{d\xi}{dw} \frac{\zeta_r\delta_i}{w} + \frac{\delta_i}{w^2} \frac{d\eta_r}{dw} \\ &\quad - \frac{\eta_r\delta_i}{w^3} - \frac{\delta_i(\zeta_r\delta_r + \zeta_i\delta_i)}{w\delta^2} \end{aligned} \quad (42)$$

There are now four free parameters:  $\alpha$ ,  $\beta$ ,  $\gamma$  and  $M$ . The quantities  $\delta_r$  and  $\delta_i$  are eigenvalues which are determined by imposing the boundary condition at the wall which is  $|\pi w M \sqrt{\gamma} - \eta| = 0$  (see Appendix B). We solved the differential equations employing a fourth order Runge-Kutta technique for trial values of  $\delta_r$  and  $\delta_i$  with the combination that satisfies the boundary condition being the eigenvalue.

$$\frac{d\pi_i}{dw} = \frac{(\delta_i\eta_r + \delta_r\eta_i)}{w} \frac{d\xi}{dw} + \frac{\eta_i}{w} + \frac{d\eta_i}{dw} - \frac{w(\zeta_i\delta_r - \zeta_r\delta_i)}{\delta^2} \quad (40)$$



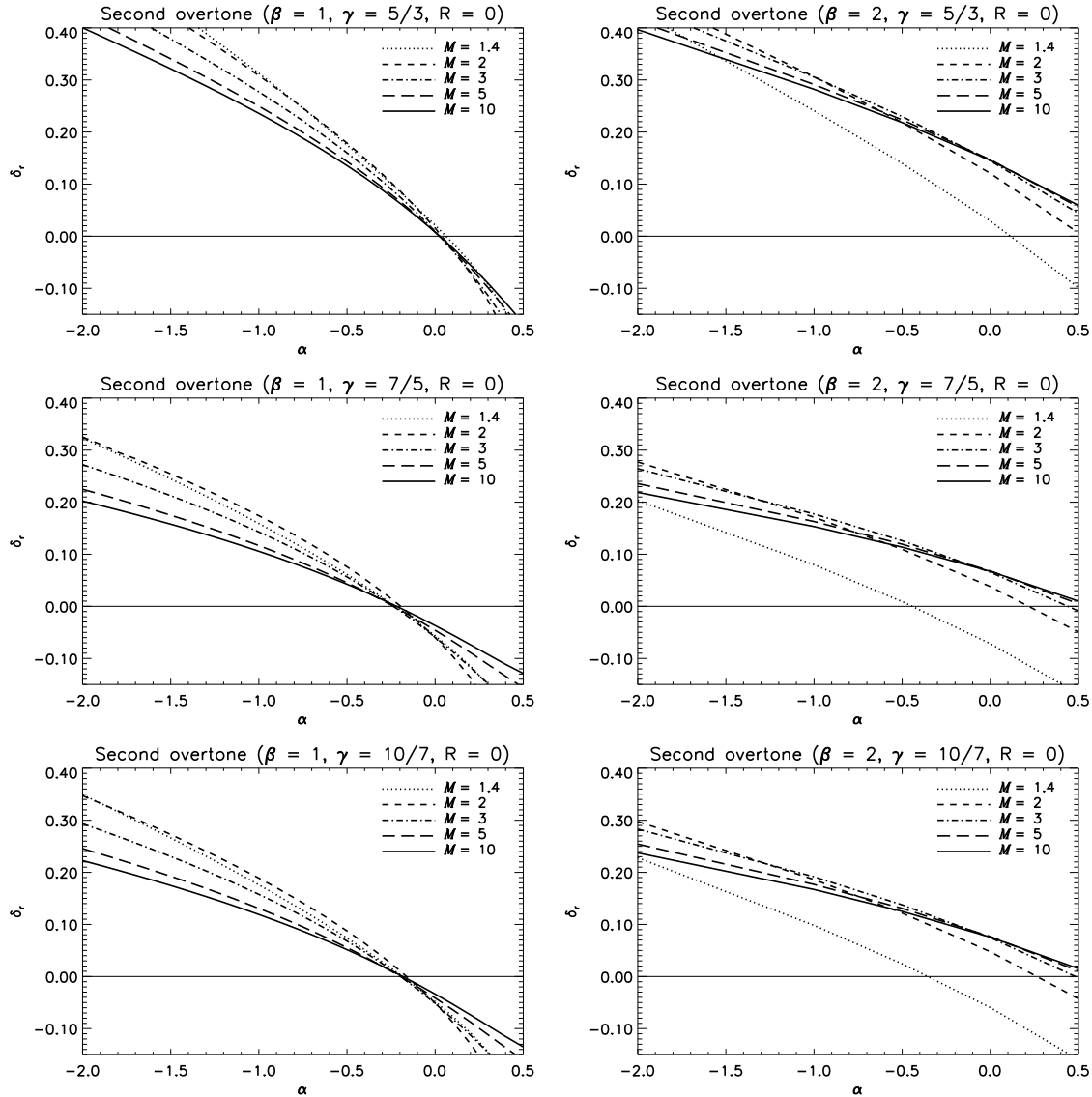


**Figure 8.** The growth/damping rates,  $\delta_r$ , as a function of  $\alpha$  for the second overtone with  $R=0$ . Values of  $\gamma$ ,  $\beta$  and  $M$  are indicated.

We followed the method described by Saxton et al. (1998) which involves choosing a grid of points in the complex plane consisting of  $\delta_r$  and  $\delta_i$  and integrating the equations for each point on the grid. The combinations that come closest to satisfying the boundary condition for each mode determine a new set of grid points with a higher resolution.

## 4 RESULTS

The main result is that a finite Mach number alters the regime of overstability as compared to the strong shock limit. However, the alteration can be in either direction.

For the standard hot atomic case, the weaker the shock, the lower the critical temperature power-law index  $\alpha_c$  below which shocks are overstable to the fundamental mode (with  $\beta = 2$  and  $\gamma = 5/3$  fixed). This case is displayed in the top-right panels of Figures 2 & 6 for the two extremes  $R = 1$  and  $R = 0$ , respectively. This is also true for the overtones (see

top-right panels of Figs. (3–5) and Figs. (7–9). Thus, the figures demonstrate that the major long wavelength modes are significantly more stable.

For the fundamental mode, the stabilising effect is of moderate significance. Even for  $M = 3$  the critical index  $\alpha_c$  is typically reduced by only 0.1–0.2 for all cases with  $R = 1$ . For the overtones, however, the stabilising effect is greater with  $\alpha_c$  reduced by  $\sim 0.4$ .

Similar results hold for the diatomic/molecular case ( $\gamma = 7/5$ ) and the molecular+helium case ( $\gamma = 10/7$ ), as illustrated in the corresponding (lower-right and middle-right) panels, for  $\beta = 2$ . The figures illustrate once again that there is no significant difference if the degrees of freedom of the helium atoms are taken into account.

Remarkably, for the  $\beta = 1$  case, the fundamental mode can grow within a wider range of  $\alpha_c$  values. That is, the shocks become more unstable due to the finite Mach number (see all the left panels of Figs. 2 & 6). This result does not hold for the overtones. The increased instability range is

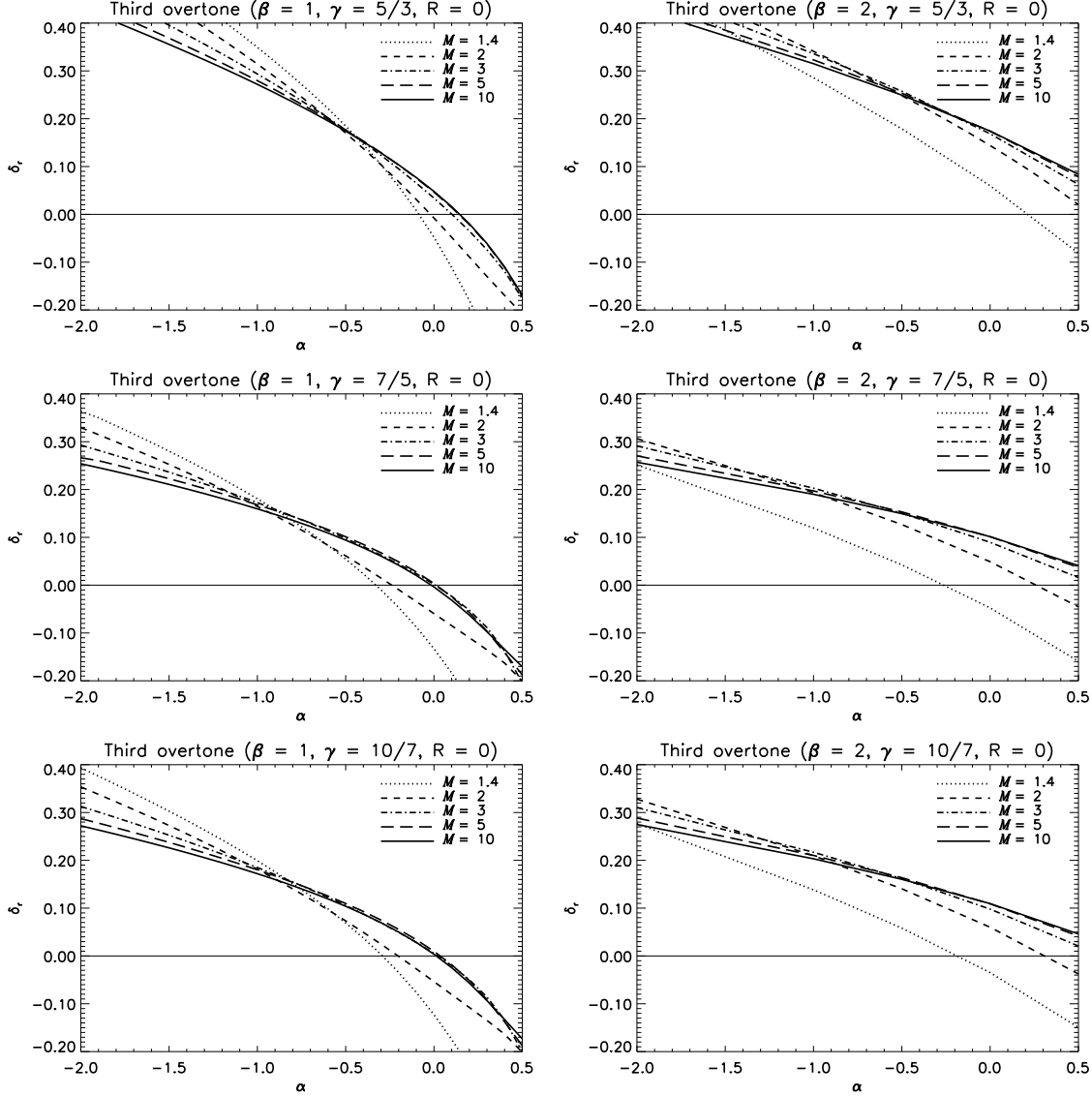


**Figure 9.** The growth/damping rates,  $\delta_r$ , as a function of  $\alpha$  for the third overtone with  $R=0$ . Values of  $\gamma$ ,  $\beta$  and  $M$  are indicated.

systematically and strongly present for the case  $R = 0$  and  $\beta = 1$  (left panels of Fig. 6). For  $R = 1$ , however, a slightly wider range exists only for moderate Mach numbers of order  $\sim 5$ .

In fact, even for  $\beta = 2$ , although the instability regime is not widened, growth rates are increased relative to the strong shock for sufficiently low/negative temperature indices  $\alpha$  (illustrated by the crossing of the loci for the growth rates in the figures). This result holds for the overtones also.

These results can be interpreted in terms of two competing physical effects. Firstly, as with the damping magnetic field, the finite Mach number cushions the shock by allowing faster sound wave propagation which should tend to smear out pressure fluctuations. In addition, for  $R = 1$ , the transmission of waves at the shell, rather than just reflection at the wall, provides a stabilising influence.

On the other hand, a reduced Mach number implies less compression and heating at the shock front. Hence, the front itself behaves in a softer fashion, analogous to a *higher*

specific heat ratio. This tends to widen the instability range of  $\alpha_c$ , as found in Paper 1. The resistance to the overstability as  $\gamma$  decreases can be interpreted as if the cooling function consisted of two components, with one component with very high  $\alpha$  located just in the hot post-shock gas. This extra cooling component (following the shock heating) produces the extra compression.

In the case of  $R = 1$ , except for the fundamental mode, the eigenfrequencies tend to have nearly the same values. The fundamental mode tends to converge for positive  $\alpha$  values for  $\beta = 1$ . For  $R = 0$  scenario, the fundamental shows a mild increase in the eigenfrequencies as  $\alpha$  increases. The overtones have almost the same frequency for  $\beta = 2$  though for  $\beta = 1$  the frequency tends to decrease with increasing  $\alpha$ .

In almost all the cases for  $\beta$  &  $\gamma$ ,  $R = 0$  scenarios have higher frequencies than  $R = 1$  as well as the eigenfrequencies seem to decrease with increasing Mach numbers.

The dependence of the overstable regimes on the mode is further explored in Figs. 18 & 19. These figures clearly

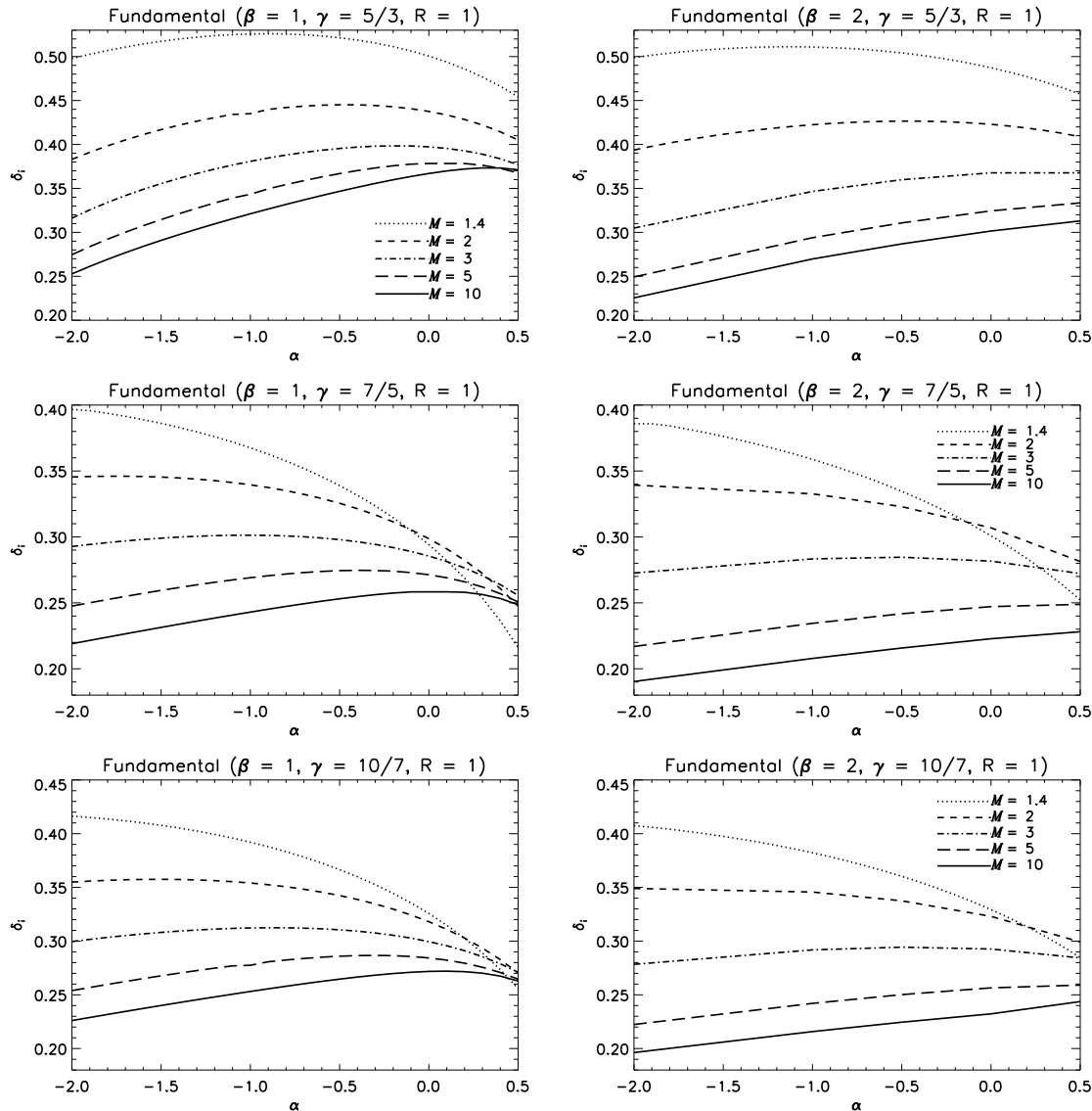


**Figure 10.** The eigenfrequency,  $\delta_i$  as a function of  $\alpha$  for the fundamental mode with  $R=1$ . Values of  $\gamma$ ,  $\beta$  and  $M$  are indicated.

show that the higher overtones are more sensitive to the Mach number. In fact, while the overtones can be exclusively present for a range in  $\alpha$  for strong shocks, the fundamental might be exclusively present for weak shocks. As an example, we can see in the case of  $M = 1.4$  ( $\beta = 2$ ,  $\gamma = 5/3$ ),  $\alpha_c = -1.031$  for the fundamental mode whereas the higher overtones have  $\alpha_c < -2$  (see also Table C13). Also this significant change in shock behaviour occurs for Mach numbers below  $\sim 3$  for the case  $R=1$  (Fig. 18) but is more complex for  $R=0$  (Fig. 19).

## 5 CONCLUSIONS

We have derived the linearised equations for one-dimensional weak shocks with general power-law cooling functions and specific heat ratios. We then solved the equations numerically and presented tables and figures which correspond to a range of conditions relevant to interstellar atomic and molec-

ular cooling processes. The two cases solved numerically are (1) cooling and accretion onto a cold stationary wall of infinite density and (2) cooling down to the pre-shock temperature. These two cases should cover most circumstances of interest for strongly radiative shocks.

We conclude that for Mach number  $M > 5$ , the strong shock overstability limits are not significantly modified. For  $M < 3$ , however, shocks are considerably more stable for most cases with the clear exception of  $\beta = 1$  and  $R = 0$  for which greater instability (of the fundamental mode) is found. The stability criterion for the overtones are more sensitive to the Mach number, which may result in a change in behaviour from overtone-dominated to fundamental-dominated as the Mach number falls below 3. These results are roughly consistent with what might be expected since the equations are altered by factors of order  $1/M^2$  in comparison to the strong shock case. We provide a possible explanation for the results in terms of a stabilis-

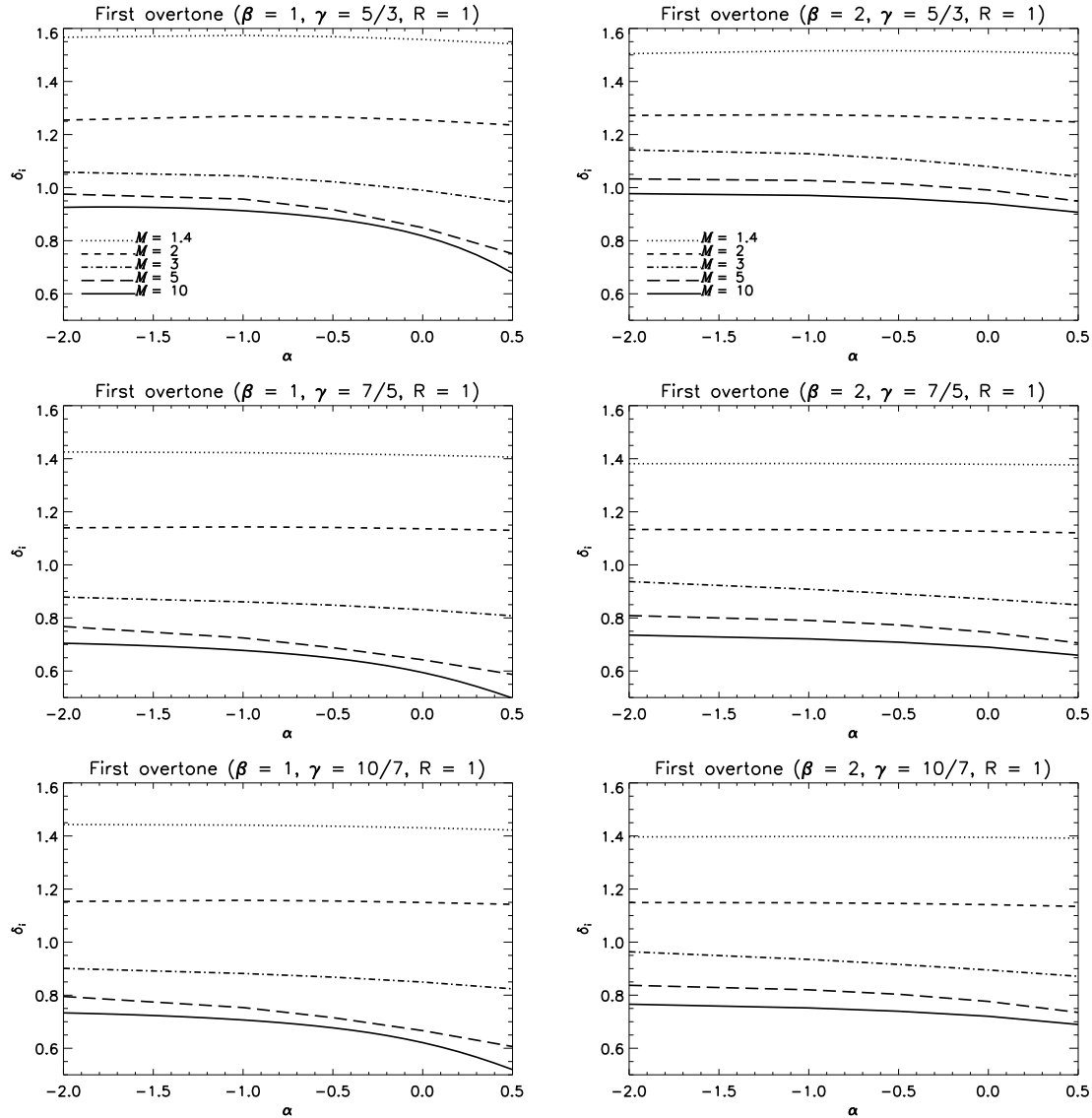


**Figure 11.** The eigenfrequency,  $\delta_i$  as a function of  $\alpha$  for the first overtone mode with  $R=1$ . Values of  $\gamma$ ,  $\beta$  and  $M$  are indicated.

ing influence provided downstream but a destabilising effect associated with the shock front.

We reach the same general conclusion derived from numerical simulations by Pittard et al. (2005) that low Mach number atomic shocks are more stable than in the strong shock limit. However, we do find different results as far as values of  $\alpha_c$  are concerned, with the numerical work uncovering a wider range of  $\alpha$  for overstability. As noted by Pittard et al. (2005), this may be due to contributions from non-linear effects in the numerical simulations. Their result is interesting especially given that the strong shock limit is closely approximated even for a Mach number of 10 (for example, the ratio of the density immediately behind the shock to the pre-shock density for a strong shock of  $\gamma = 5/3$  is 4 in table 1 of Pittard et al. (2005)). Our instability results reveal that the stability criterion is very close to the standard  $\alpha_c \sim 0.4$  even for a Mach number of 10 (see Table C13). We thus find our linear instability results not to be surprising

in the sense that the strong shock results are attained very much as expected from the Rankine-Hugoniot conditions.

In terms of shock speeds, our results imply that the stability regime for shock propagation into an interstellar atomic medium of temperature  $\sim 10,000$  K must take into account the finite Mach number only for  $v < 50$  km s $^{-1}$ . However, such shocks are in any case expected to be stable due to the steep temperature dependence of the cooling function. Only if the pre-shock temperature is several times higher than 10,000 K, can we expect behaviour modified from the strong shock limit, as discussed in detail by Pittard et al. (2005).

A further regime of interest is that of the propagation of radiative shocks into cool atomic media. Shock waves of speed 10–15 km s $^{-1}$  heat atomic gas to temperatures 2,900 K–6,500 K. Then, fine-structure cooling of elements such as C $^{+}$  and Fe $^{+}$  dominates the cooling with cooling functions that may increase as the temperature falls even in scenarios involving non-equilibrium ionisation

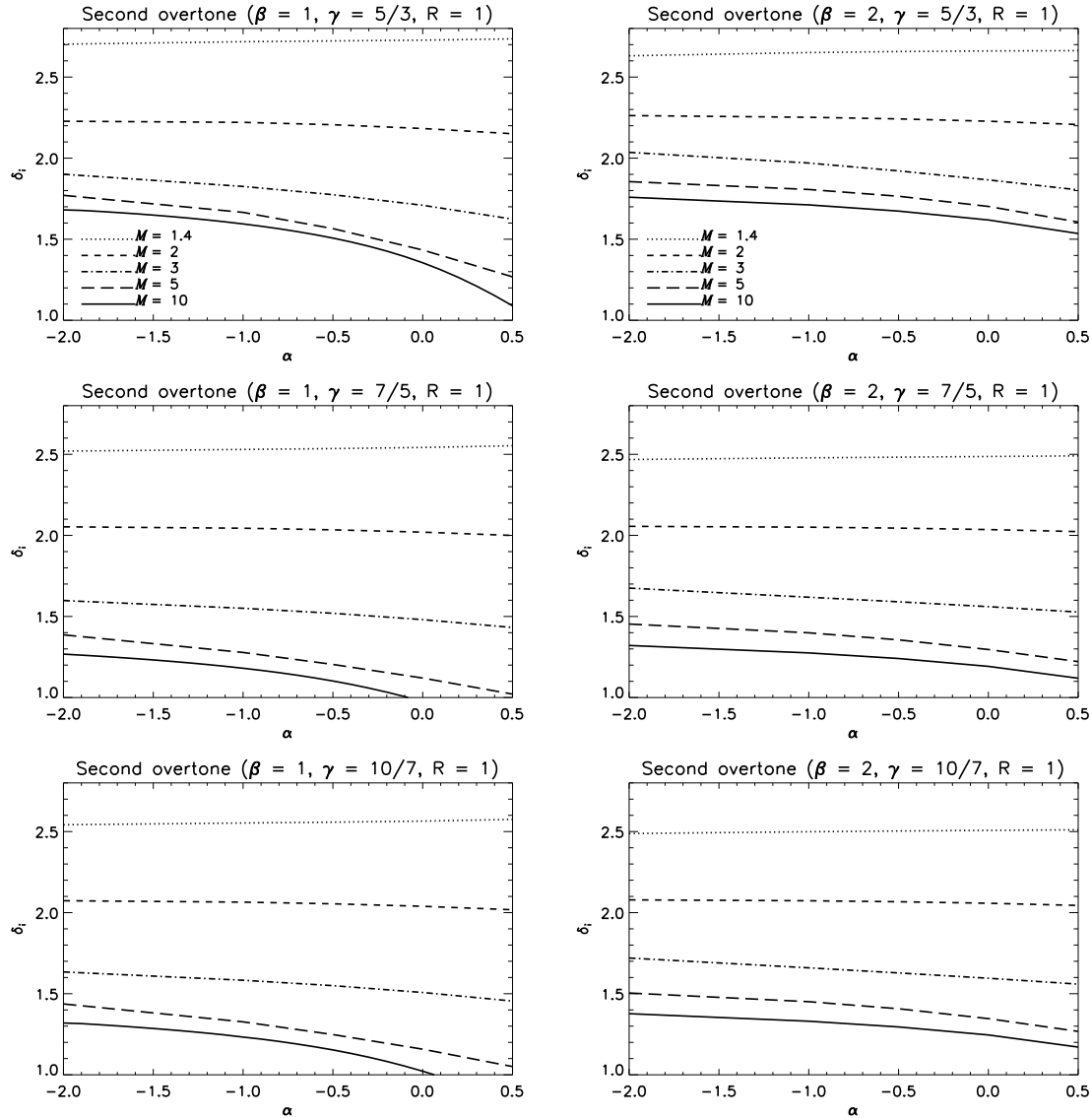


**Figure 12.** The eigenfrequency,  $\delta_i$  as a function of  $\alpha$  for the second overtone mode with  $R = 1$ . Values of  $\gamma$ ,  $\beta$  and  $M$  are indicated.

(Dalgarno & McCray 1972). Our analysis indicates that such shocks are overstable to the fundamental mode even at Mach numbers as low as 3 e.g. even if the temperature in the pre-shock medium is over 1000 K. These shocks possess thick radiative layers with relatively long cooling times (of order  $10^5/n$  yr) and correspondingly long growth and non-linear oscillation periods.

For molecular shocks into cold gas, only extremely low speed shocks will possess a low Mach number (e.g.  $v < 1 \text{ km s}^{-1}$ ). Furthermore, we expect the magnetic field to provide a greater influence on the stability criterion as reported in Paper II. For example, an Alfvén (Mach) number of less than 20 will stabilise the fundamental and first three harmonics for all  $\alpha$  greater than zero (taking  $\beta = 2$ ). To achieve the same stability without the magnetic field, requires a Mach number of  $M < 4$  for  $R = 1$  and  $M < 1.7$  for  $R = 0$ . Note, however, that we have assumed a transverse magnetic field in Paper II.

The combined results of this series of papers indicate

that slow molecular jump shocks are generally not overstable to the longest-wavelength fundamental mode since molecular cooling functions tend to be steep positive functions of temperature (see Paper I). The overtones, however, may be responsible for variability which we suggest will take the form of low-amplitude jittering. However, it should be remarked that other hydrodynamic processes involving the dense shell (Vishniac 1994) or turbulence in the pre-shock medium (Sutherland et al. 2003) may also drive linear or non-linear instabilities.

Dissociative shocks possess complex time-dependent cooling and chemistry within the radiative layer and numerical simulations are necessary to determine the stability properties (Smith & Rosen 2003; Lesaffre et al. 2004). In any case, the possibility to observe the implied quasi-periodic variations depends on the resolution of the observing instrument and the length of coherence across a shock front to the oscillations. However, even with low resolution, the development of density structure will still

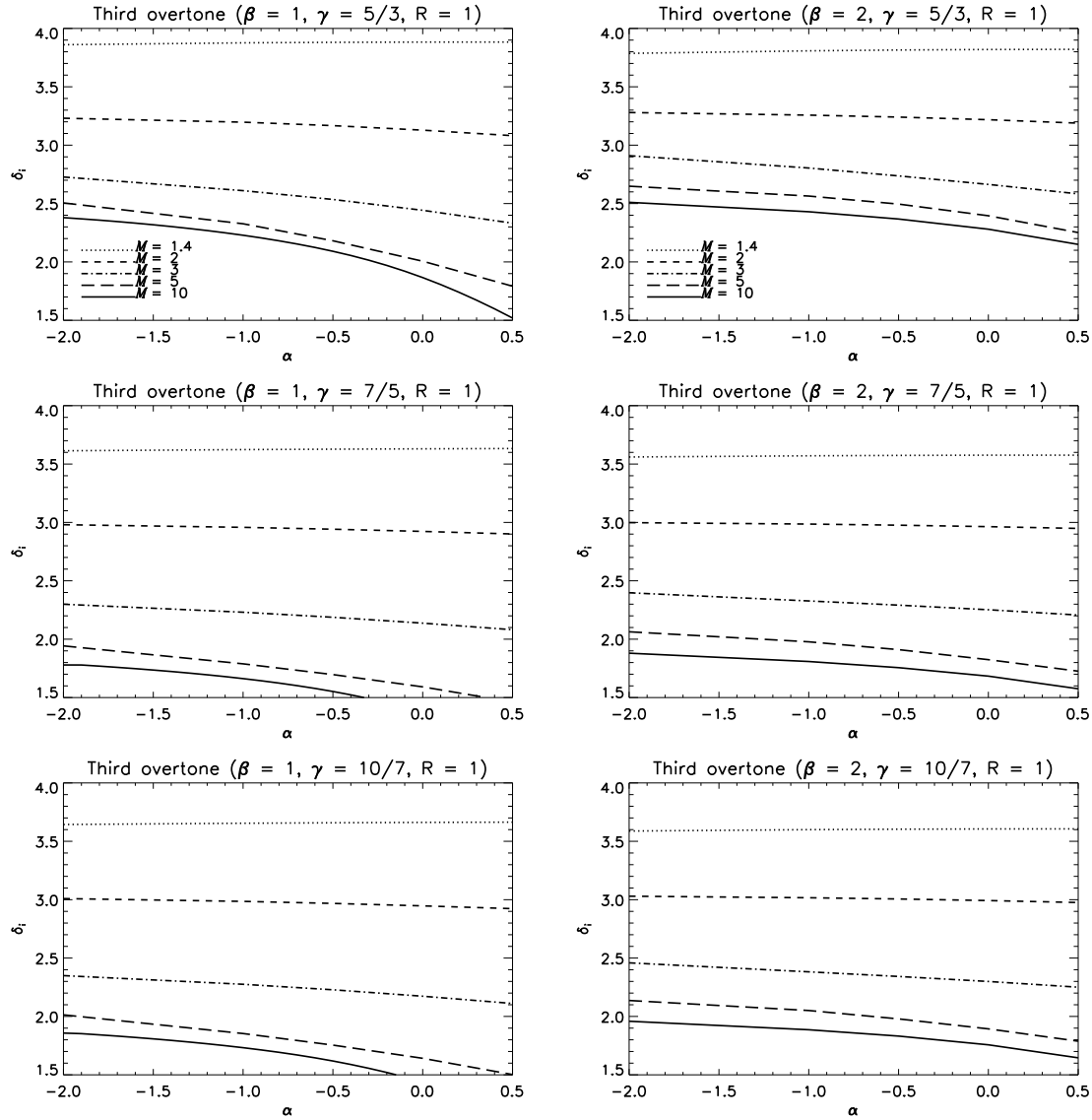


**Figure 13.** The eigenfrequency,  $\delta_i$  as a function of  $\alpha$  for the third overtone mode with  $R=1$ . Values of  $\gamma$ ,  $\beta$  and  $M$  are indicated.

produce shock signatures inconsistent with steady shock models (Sutherland et al. 2003). A similar conclusion was drawn from multi-dimensional simulations of C-type molecular shocks in which ion-neutral streaming generates an instability (Mac Low & Smith 1997).

## ACKNOWLEDGMENTS

Research at Armagh Observatory is funded by the Department of Culture, Arts and Leisure, Northern Ireland. BR is extremely grateful to Sathya Sai Baba for encouragement and also thanks Professor S. Kandaswami for guidance.

## REFERENCES

- Bertschinger E., 1986, *ApJ*, 304, 154  
 Chevalier R. A., Imamura J. N., 1982, *ApJ*, 261, 543  
 Dalgarno A., McCray R. A., 1972, *ARA&A*, 10, 375  
 Dgani R., Soker N., 1994, *ApJ*, 434, 262  
 Draine B. T., McKee C. F., 1993, *ARA&A*, 31, 373  
 Imamura J. N., Aboasha A., Wolff M. T., Wood K. S., 1996, *ApJ*, 458, 327  
 Imamura J. N., Wolff M. T., Durisen R. H., 1984, *ApJ*, 276, 667  
 Langer S. H., Chanmugam G., Shaviv G., 1981, *ApJ*, 245, L23  
 Lesaffre P., Chièze J.-P., Cabrit S., Pineau des Forêts G., 2004, *A&A*, 427, 147  
 Mac Low M.-M., Smith M. D., 1997, *ApJ*, 491, 596  
 Pittard J. M., Dobson M. S., Durisen R. H., Dyson J. E., Hartquist T. W., O'Brien J. T., 2005, *A&A*, 438, 11  
 Priest E. R., 1982, *Solar magneto-hydrodynamics*. Dordrecht, Holland ; Boston : D. Reidel Pub. Co. ; Hingham,  
 Ramachandran B., Smith M. D., 2005a, *MNRAS*, 362, 1353  
 Ramachandran B., Smith M. D., 2005b, *MNRAS*, 357, 707  
 Saxton C. J., Wu K., Pongracic H., Shaviv G., 1998, *MN-*

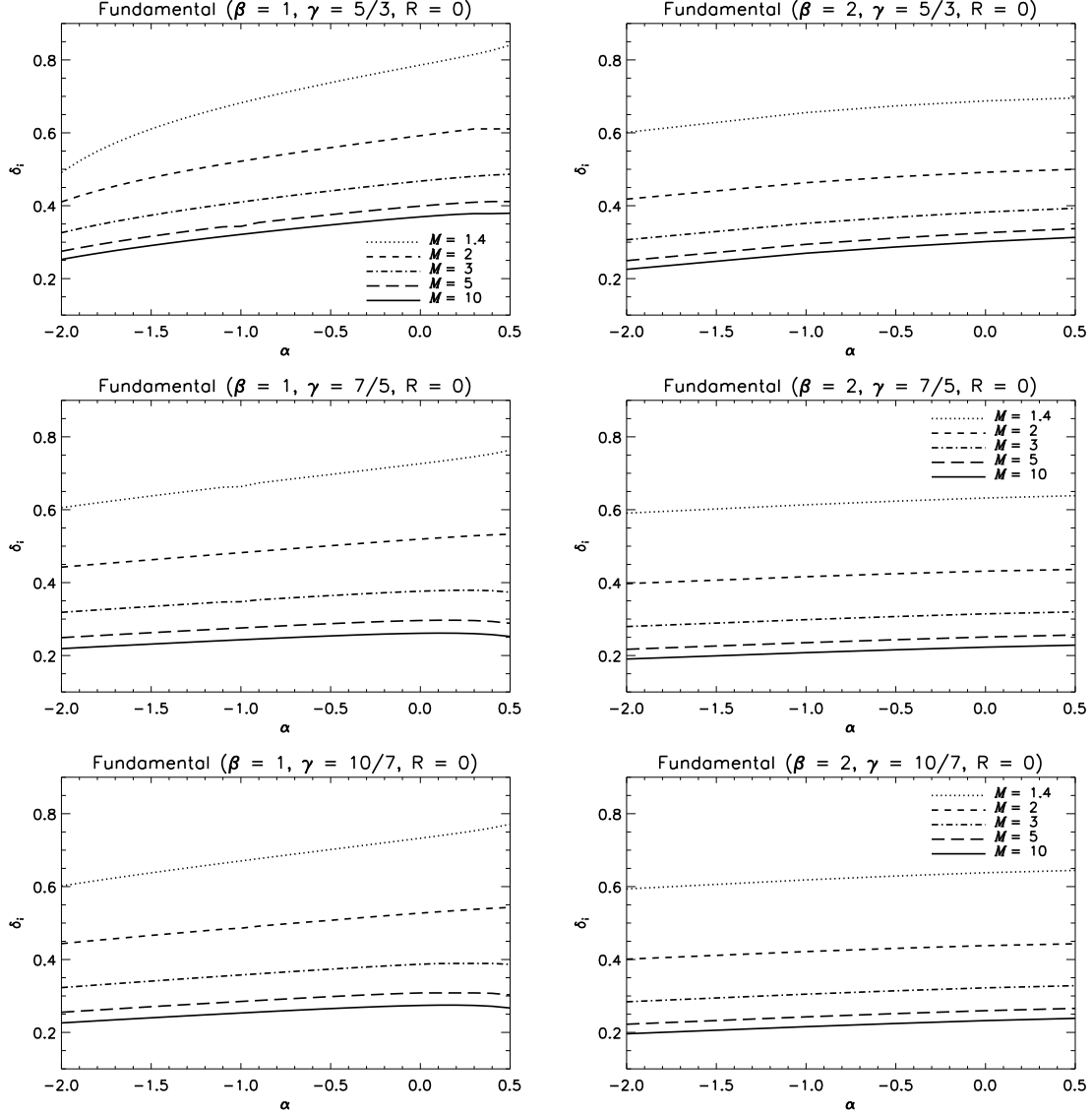


**Figure 14.** The eigenfrequency,  $\delta_i$  as a function of  $\alpha$  for the fundamental mode with  $R=0$ . Values of  $\gamma$ ,  $\beta$  and  $M$  are indicated.

- RAS, 299, 862  
 Shore S. N., 1993, An introduction to astrophysical hydrodynamics. Academic Press  
 Shull J. M., Draine B. T., 1987, in ASSL Vol. 134: Interstellar Processes The physics of interstellar shock waves. pp 283–319  
 Smith M. D., Rosen A., 2003, MNRAS, 339, 133  
 Strickland R., Blondin J. M., 1995, ApJ, 449, 727  
 Sutherland R. S., Bicknell G. V., Dopita M. A., 2003, ApJ, 591, 238  
 Toth G., Draine B. T., 1993, ApJ, 413, 176  
 Vishniac E. T., 1994, ApJ, 428, 186

## APPENDIX A: BOUNDARY CONDITIONS AT THE MOVING SHOCK

In the steady state case, both the incoming gas and the outgoing gas (at the shock) are the same for a stationary

observer as well as the shock. But the situation changes when the shock starts oscillating. Now the stationary observer will find the same incoming velocity with a different velocity for the post-shock gas which consists of two parts, viz, the steady state velocity and a small perturbed term which will be determined as follows. Let the velocity of the shock be  $v_s = v_{s1}e^{\sigma t}$  according to the stationary observer. In the frame of the shock,

$$v_{in} = -u_{in} - v_s, \quad (\text{A1})$$

where  $v_{in}$  is the incoming gas velocity. There will be a small perturbation to the Mach number and the new Mach number ( $M_n$ ) is written as  $M_n = M + M_1$ , where  $M_1 = \frac{v_s}{c_s}$  and  $M_1 \ll M$ . Here  $c_s$  is the velocity of sound. If  $v$  is the velocity of the post-shock gas in the observer frame, it implies that  $v - v_s$  will be the velocity as seen from the shock frame. Applying the Rankine-Hugoniot condition, we obtain

$$v - v_s = \left[ \frac{(\gamma - 1) M_n^2 + 2}{(\gamma + 1) M_n^2} \right] v_{in} \quad (\text{A2})$$

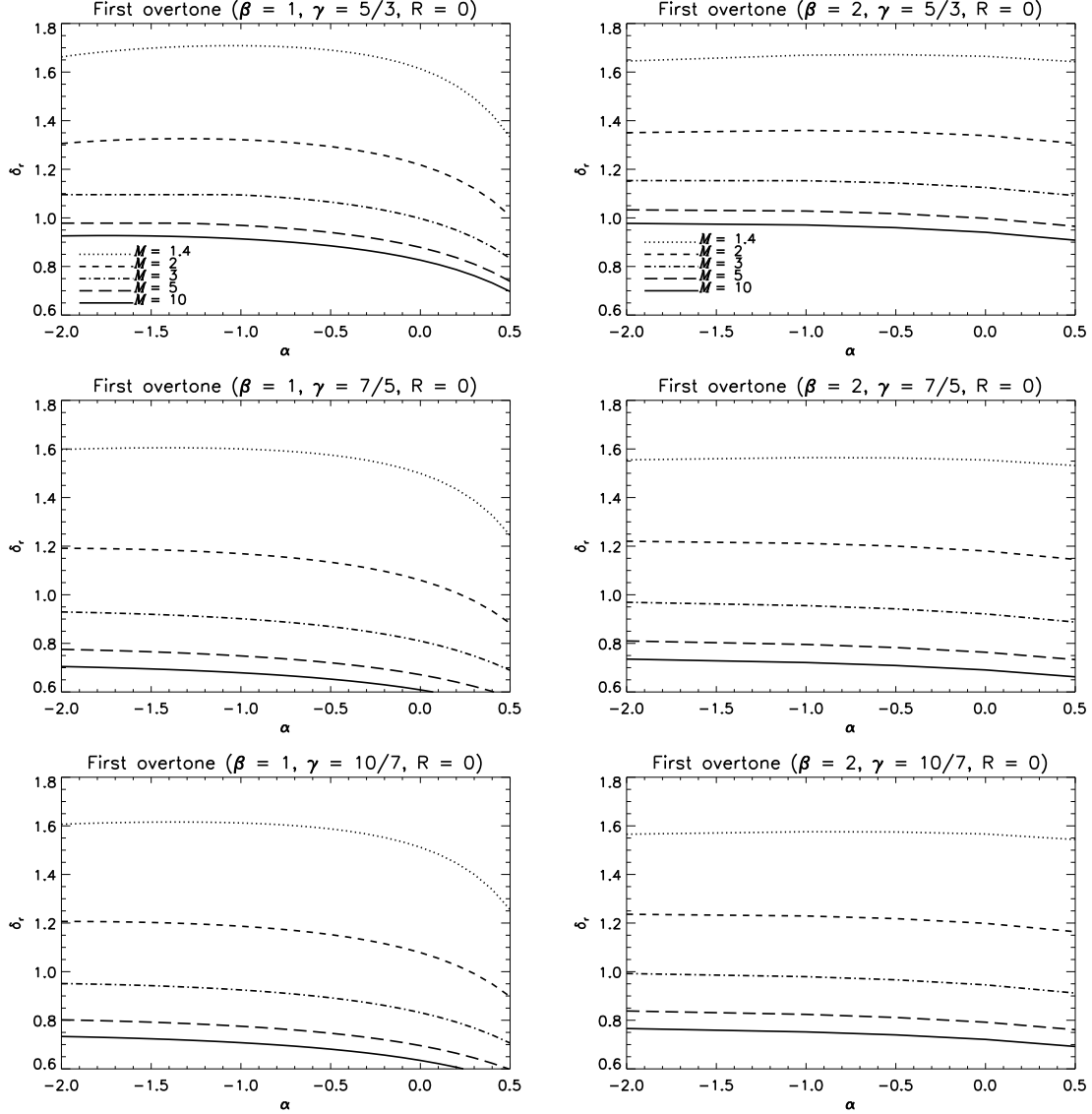


**Figure 15.** The eigenfrequency,  $\delta_i$  as a function of  $\alpha$  for the first overtone mode with  $R=0$ . Values of  $\gamma$ ,  $\beta$  and  $M$  are indicated.

Rearranging the terms, we obtain

$$v = - \left[ \frac{(\gamma-1) M^2 + 2}{(\gamma+1) M^2} \right] u_{in} + \frac{2v_s}{\gamma+1} \left[ 1 + \frac{1}{M^2} \right]. \quad (\text{A3})$$

Comparing this with equations (5) and (25) we find that the perturbed velocity is

$$v_1 = \frac{2v_{s1}}{\gamma+1} \left[ 1 + \frac{1}{M^2} \right]. \quad (\text{A4})$$

Now for the perturbation in density, we use the Rankine-Hugoniot condition which expresses the conservation of mass, viz,

$$\rho_{in} v_{in} = \rho (v - v_s), \quad (\text{A5})$$

where  $\rho_{in}$  and  $\rho$  are the pre-shock and post-shock densities and  $\rho_{in} = \rho_a$ . Simplifying, we get

$$\rho = \left[ \frac{(\gamma+1) M^2}{(\gamma-1) M^2 + 2} \right] \rho_a + \left[ \frac{4v_s \rho_a (\gamma+1) M^2}{u_{in} [2 + (\gamma-1) M^2]^2} \right] \quad (\text{A6})$$

which implies from equations (4) and (23) that the density perturbation is

$$\rho_1 = \left[ \frac{4v_{s1} \rho_a (\gamma+1) M^2}{u_{in} [2 + (\gamma-1) M^2]^2} \right]. \quad (\text{A7})$$

For the pressure perturbation, we use the Rankine-Hugoniot condition for the conservation of momentum flux. Denoting  $P$  as the post-shocked gas pressure,

$$P = \rho_{in} v_{in}^2 - \rho (v - v_s)^2 + P_{in}, \quad (\text{A8})$$

where  $P_{in} = P_a$  is the pre-shock thermal pressure. Solving the above equation results in

$$P = P_0 + \frac{4\rho_{in} u_{in} v_s}{\gamma+1}, \quad (\text{A9})$$

which implies from equation (24) that the perturbed part of the pressure is

$$P_1 = \left( \frac{4\rho_a u_{in} v_{s1}}{\gamma+1} \right). \quad (\text{A10})$$



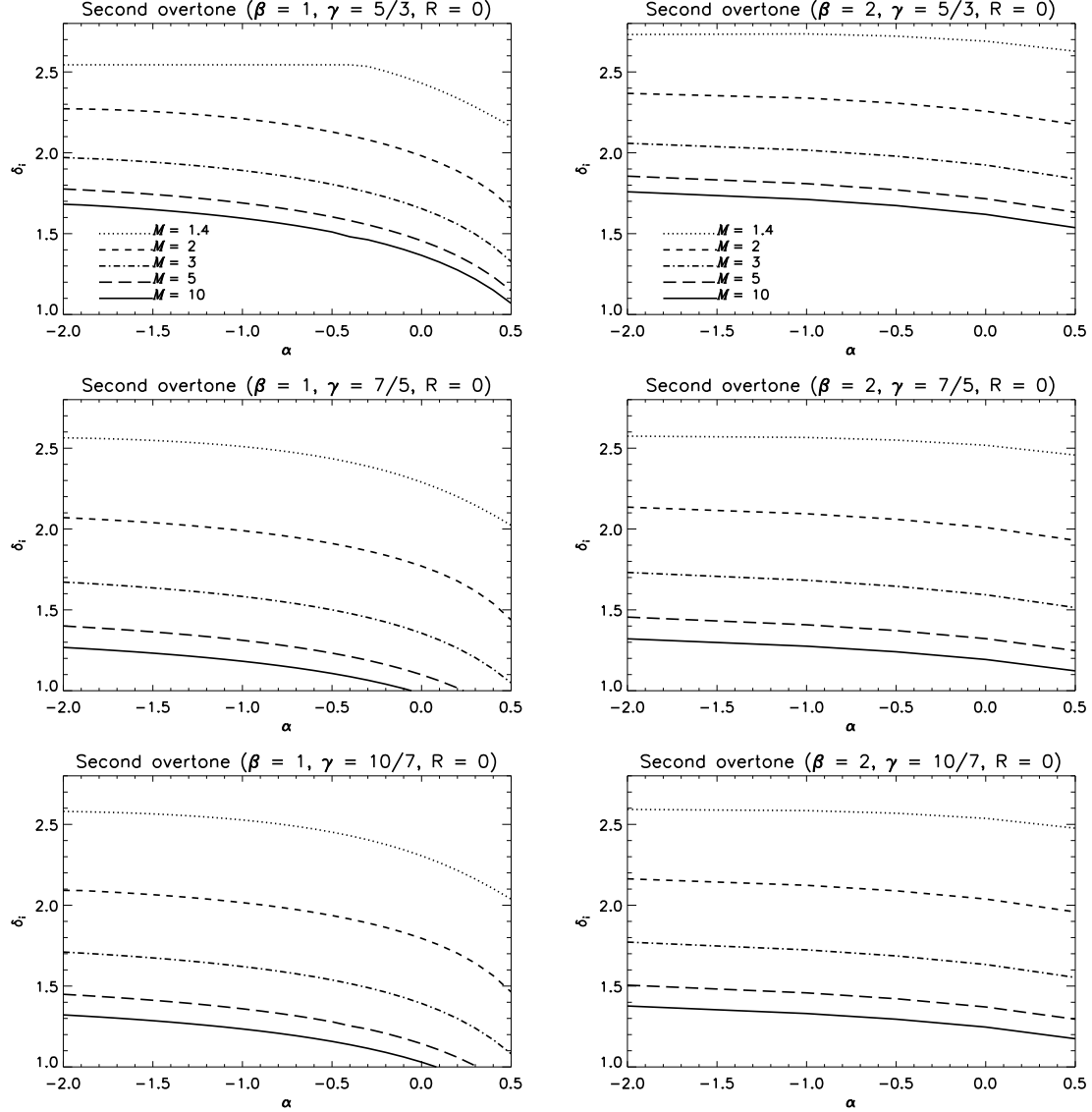


Figure 16. The eigenfrequency,  $\delta_i$  as a function of  $\alpha$  for the second overtone with  $R = 0$ . Values of  $\gamma$ ,  $\beta$  and  $M$  are indicated.

## APPENDIX B: BOUNDARY CONDITION AT THE SHELL DURING THE SHOCK OSCILLATIONS

At the shell we consider the two scenarios. One case is when the temperature goes to zero. The second is when the temperature of the fluid cools down to the pre-shock temperature.

The first scenario is very simple as the pressure goes to zero, the density becomes infinite and therefore the velocity goes to zero which implies the velocity perturbation also vanishes at  $w = 0$ . Therefore,

$$\eta = 0 \quad (\text{B1})$$

The boundary condition for the second case is evaluated

as follows. We represent the physical quantities as

$$\rho = \rho_0 + \rho_1 e^{i(ft+kx)}, \quad (\text{B2})$$

$$P = P_0 + P_1 e^{i(ft+kx)}, \quad (\text{B3})$$

$$v = v_0 + v_1 e^{i(ft+kx)}, \quad (\text{B4})$$

where  $k$  is the wavenumber, which represents the direction of the outgoing wave towards the shell and  $f$  is the frequency. The above equations are substituted in (1) and (2) to yield

$$\frac{f}{k} = - \left( \frac{\rho_0 v_1 v_0 + P_1}{\rho_0 v_1} \right), \quad (\text{B5})$$

$$\frac{f}{k} = - \left( \frac{\rho_0 v_1 + \rho_1 v_0}{\rho_1} \right). \quad (\text{B6})$$

Equating the above expressions leads to

$$P_1 = \frac{\rho_0^2 v_1^2}{\rho_1}. \quad (\text{B7})$$

Now the pressure perturbation can also be expressed in

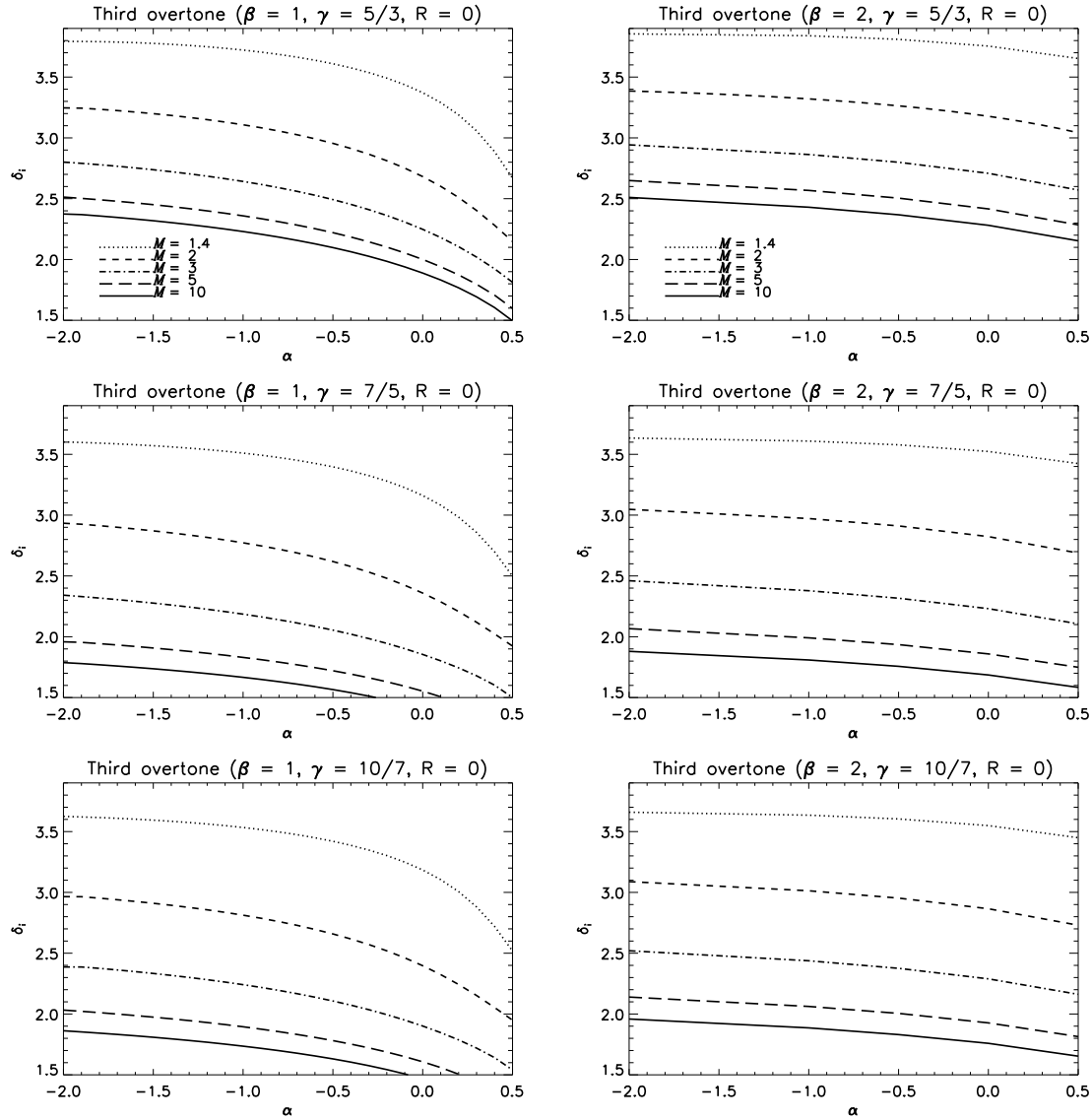


**Figure 17.** The eigenfrequency,  $\delta_i$  as a function of  $\alpha$  for the third overtone with  $R=0$ . Values of  $\gamma$ ,  $\beta$  and  $M$  are indicated.

terms of the density perturbation by

$$P_1 = \frac{c_s^2 \rho_1}{\gamma}. \quad (\text{B8})$$

Equations (B7) and (B8) yield the boundary condition at the shell as

$$P_1 = -\frac{c_s v_1 \rho_0}{\sqrt{\gamma}}. \quad (\text{B9})$$

The minus sign indicates the direction of the gas flow. Note that the perturbed quantities are functions of  $x$ , which itself is a function of  $\xi$  from (20). The expression (B9) can be written in terms of the non-dimensional quantities as

$$\pi = \frac{\eta}{wM\sqrt{\gamma}}. \quad (\text{B10})$$

The above quantities are evaluated at the shell boundary  $w = -\frac{1}{\gamma M^2}$ .

## APPENDIX C: TABLES

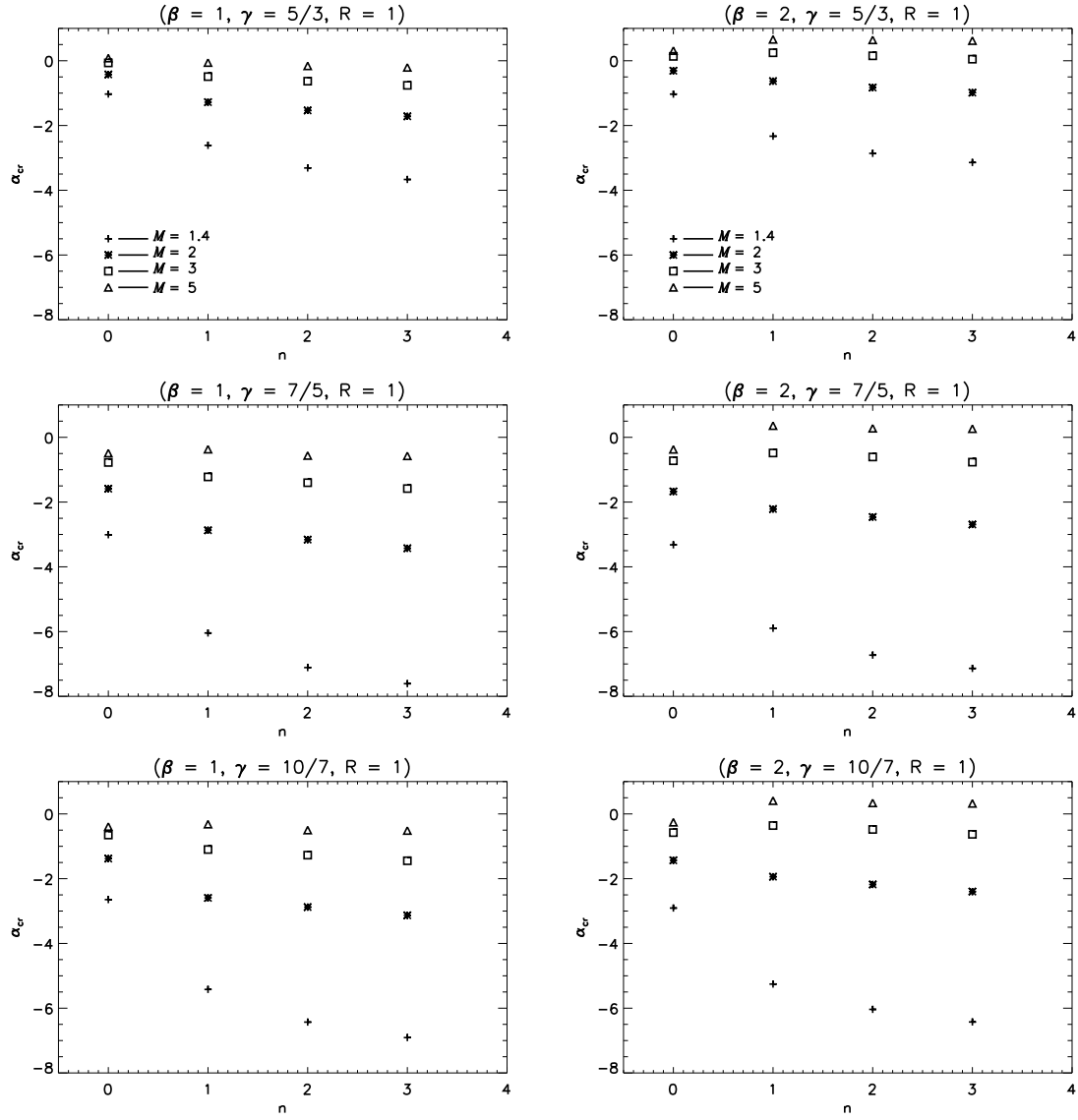


**Figure 18.** The critical values of  $\alpha$  plotted against the overtones for the displayed values of  $\gamma$ ,  $\beta$  and  $M$ , with  $R = 1$ .

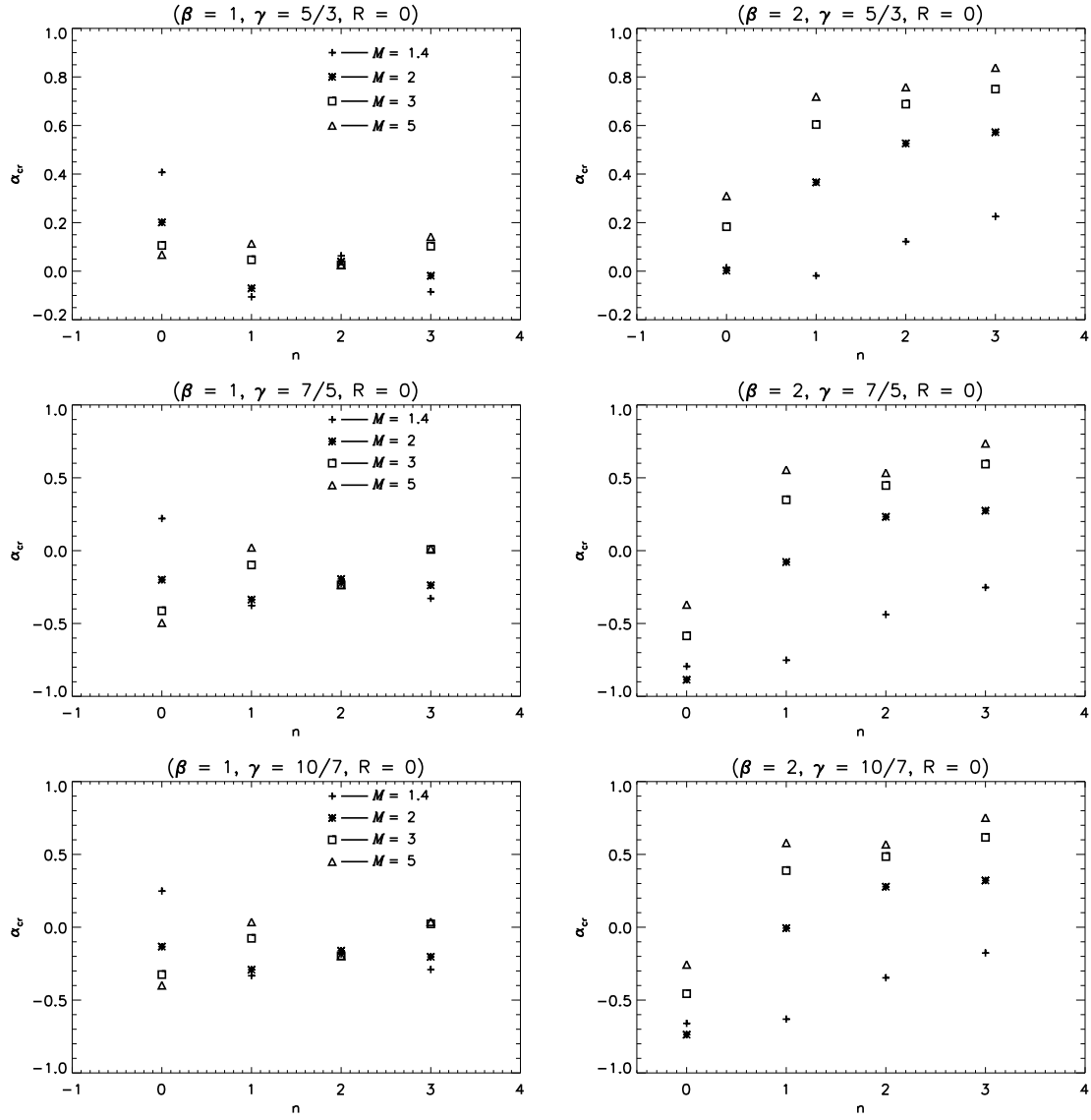


**Figure 19.** The critical values of  $\alpha$  plotted against the overtones for the displayed values of  $\gamma$ ,  $\beta$  and  $M$  with  $R = 0$ .

**Table C1.** Growth rates ( $\delta_r$ ) for several modes and Mach number  $M$ , for  $\gamma = 5/3$ ,  $\beta = 1$ ,  $R = 1$

fundamental							first overtone					
$\alpha$	M = 1.4	M = 2	M = 3	M = 5	M = 10	M = 40	M = 1.4	M = 2	M = 3	M = 5	M = 10	M = 40
-2	0.15868	0.25826	0.28033	0.24792	0.22699	0.22036	-0.11795	0.15932	0.35105	0.37958	0.36678	0.36174
-1	-0.00505	0.09883	0.14289	0.13754	0.12761	0.12418	-0.32850	-0.06753	0.13312	0.21459	0.21670	0.21518
-0.5	-0.09487	0.01371	0.07180	0.08018	0.07432	0.07209	-0.44397	-0.19630	0.00248	0.11434	0.13225	0.13237
0.0	-0.19324	-0.08116	-0.01084	0.01266	0.00988	0.00782	-0.56824	-0.33770	-0.14700	-0.01762	0.03008	0.03384
0.5	-0.30449	-0.19182	-0.11488	-0.07983	-0.08218	-0.09264	-0.70485	-0.49642	-0.31672	-0.18944	-0.10965	-0.08814

second overtone						third overtone						
$\alpha$	M = 1.4	M = 2	M = 3	M = 5	M = 10	M = 40	M = 1.4	M = 2	M = 3	M = 5	M = 10	M = 40
-2	-0.25737	0.11634	0.38202	0.42270	0.40013	0.39208	-0.33910	0.07365	0.36575	0.44685	0.43170	0.42569
-1	-0.47626	-0.14414	0.11445	0.23892	0.23577	0.23124	-0.57060	-0.19824	0.07725	0.25465	0.27575	0.26912
-0.5	-0.59555	-0.28836	-0.04255	0.11200	0.13569	0.13299	-0.69855	-0.34409	-0.08671	0.10793	0.17270	0.17295
0.0	-0.72470	-0.44442	-0.21268	-0.05955	0.00642	0.00826	-0.84003	-0.49686	-0.25940	-0.08286	0.03531	0.04801
0.5	-0.86990	-0.62068	-0.39328	-0.25618	-0.18312	-0.16055	-1.00563	-0.66103	-0.43953	-0.28837	-0.19206	-0.16239

**Table C2.** Eigenfrequencies ( $\delta_i$ ) for several modes and Mach number  $M$ , for  $\gamma = 5/3$ ,  $\beta = 1$ ,  $R = 1$ .

fundamental							first overtone					
$\alpha$	M = 1.4	M = 2	M = 3	M = 5	M = 10	M = 40	M = 1.4	M = 2	M = 3	M = 5	M = 10	M = 40
-2	0.49769	0.38303	0.31619	0.27455	0.25269	0.24564	1.56673	1.25451	1.05821	0.97571	0.92570	0.90878
-1	0.52576	0.43733	0.38095	0.34452	0.32110	0.31276	1.57364	1.26951	1.04417	0.95685	0.91306	0.89573
-0.5	0.52151	0.44530	0.39563	0.36700	0.34674	0.33839	1.56899	1.26603	1.02228	0.91709	0.88295	0.86733
0.0	0.50074	0.43772	0.39748	0.37900	0.36711	0.36009	1.55840	1.25445	0.98989	0.84925	0.81847	0.80948
0.5	0.45451	0.40529	0.37720	0.36932	0.37161	0.36932	1.54192	1.23597	0.94367	0.75097	0.67845	0.68130

second overtone						third overtone						
$\alpha$	M = 1.4	M = 2	M = 3	M = 5	M = 10	M = 40	M = 1.4	M = 2	M = 3	M = 5	M = 10	M = 40
-2	2.70280	2.22769	1.90067	1.77063	1.68329	1.65287	3.86044	3.23086	2.72743	2.50555	2.37952	2.33633
-1	2.71810	2.22077	1.82547	1.66545	1.59446	1.56459	3.87656	3.19712	2.61057	2.32686	2.17500	2.18843
-0.5	2.72290	2.20614	1.77467	1.56552	1.50713	1.48020	3.88092	3.16737	2.53515	2.18114	2.09166	2.05832
0.0	2.72760	2.18283	1.70942	1.43350	1.35523	1.33649	3.88313	3.12860	2.44235	2.00621	1.86671	1.85210
0.5	2.73585	2.15068	1.62404	1.26813	1.08860	1.04335	3.88372	3.08166	2.33224	1.79238	1.51808	1.45950

**Table C3.** Growth rates ( $\delta_r$ ) for several modes and Mach number  $M$ , for  $\gamma = 5/3$ ,  $\beta = 2$ ,  $R = 1$ .

fundamental							first overtone					
$\alpha$	M = 1.4	M = 2	M = 3	M = 5	M = 10	M = 40	M = 1.4	M = 2	M = 3	M = 5	M = 10	M = 40
-2	0.13189	0.19818	0.19427	0.17816	0.16996	0.16729	-0.05599	0.26403	0.36978	0.35914	0.34838	0.34456
-1	-0.00441	0.08220	0.10656	0.10601	0.10393	0.10314	-0.23776	0.07674	0.23030	0.24461	0.24104	0.23943
-0.5	-0.07480	0.02392	0.06172	0.06845	0.06920	0.06929	-0.33698	-0.02827	0.14980	0.18295	0.18330	0.18277
0.0	-0.14797	-0.03902	0.01365	0.02775	0.03128	0.03225	-0.44318	-0.14382	0.05429	0.11407	0.11948	0.12011
0.5	-0.22489	-0.10672	-0.04008	-0.01808	-0.01208	-0.01027	-0.55801	-0.27239	-0.06258	0.03129	0.04564	0.04752
1	-0.30666	-0.18195	-0.10297	-0.07202	-0.06450	-0.06236	-0.68424	-0.41747	-0.20578	-0.08035	-0.05461	-0.04217

second overtone							third overtone					
$\alpha$	M = 1.4	M = 2	M = 3	M = 5	M = 10	M = 40	M = 1.4	M = 2	M = 3	M = 5	M = 10	M = 40
-2	-0.15510	0.26401	0.43286	0.41340	0.39665	0.39089	-0.21458	0.24211	0.46031	0.44702	0.43150	0.42621
-1	-0.35234	0.04138	0.27046	0.29083	0.28211	0.27884	-0.42111	0.00388	0.27767	0.32220	0.31513	0.31229
-0.5	-0.45919	-0.08191	0.16733	0.22224	0.21822	0.21620	-0.53220	-0.12642	0.15723	0.25036	0.24933	0.24775
0.0	-0.57278	-0.21457	0.04229	0.14228	0.14578	0.14508	-0.64969	-0.26471	0.01475	0.16249	0.17412	0.17392
0.5	-0.69484	-0.35772	-0.10506	0.03762	0.05945	0.06016	-0.77540	-0.41129	-0.14643	0.03791	0.08229	0.08503
1	-0.82860	-0.51344	-0.27149	-0.11390	-0.05243	-0.04859	-0.91289	-0.56741	-0.32169	-0.14084	-0.04348	-0.03113

**Table C4.** Eigenfrequencies ( $\delta_i$ ) for several modes and Mach number  $M$ , for  $\gamma = 5/3$ ,  $\beta = 2$ ,  $R = 1$ .

fundamental							first overtone					
$\alpha$	M = 1.4	M = 2	M = 3	M = 5	M = 10	M = 40	M = 1.4	M = 2	M = 3	M = 5	M = 10	M = 40
-2	0.49898	0.39376	0.30489	0.24931	0.22545	0.21802	1.50492	1.27215	1.14203	1.03289	0.97737	0.95930
-1	0.51095	0.42256	0.34659	0.29390	0.26972	0.26210	1.51568	1.27464	1.12782	1.02682	0.97073	0.95221
-0.5	0.50429	0.42670	0.35989	0.31075	0.28687	0.27922	1.51588	1.26981	1.10822	1.01444	0.95975	0.94120
0.0	0.48748	0.42303	0.36770	0.32441	0.30149	0.29389	1.51247	1.26093	1.07935	0.99119	0.94052	0.92221
0.5	0.45759	0.40898	0.36773	0.33358	0.31304	0.30569	1.50540	1.24721	1.04134	0.94920	0.90708	0.88992
1	0.40896	0.37941	0.35502	0.33407	0.31902	0.31254	1.49504	1.22768	0.99372	0.87684	0.84445	0.83179

second overtone							third overtone					
$\alpha$	M = 1.4	M = 2	M = 3	M = 5	M = 10	M = 40	M = 1.4	M = 2	M = 3	M = 5	M = 10	M = 40
-2	2.63136	2.26258	2.03580	1.85521	1.75898	1.72734	3.78642	3.27964	2.91024	2.64871	2.51055	2.46531
-1	2.65103	2.25191	1.96991	1.80674	1.71169	1.67991	3.80807	3.25744	2.80433	2.56425	2.42987	2.38504
-0.5	2.65732	2.24193	1.92143	1.76504	1.67351	1.64191	3.81513	3.24056	2.73687	2.49563	2.36767	2.32344
0.0	2.66122	2.22764	1.86580	1.70217	1.61873	1.58778	3.81947	3.21813	2.66391	2.39541	2.28046	2.23764
0.5	2.66295	2.20739	1.80436	1.60594	1.53512	1.50635	3.82104	3.18878	2.58310	2.25152	2.15010	2.11156
1	2.66331	2.17960	1.73345	1.47113	1.39343	1.37162	3.81994	3.15190	2.48765	2.06884	1.93489	1.90926

**Table C5.** Growth rates ( $\delta_r$ ) for several modes and Mach number  $M$ , for  $\gamma = 7/5$ ,  $\beta = 1$ ,  $R = 1$ .

fundamental							first overtone					
$\alpha$	M = 1.4	M = 2	M = 3	M = 5	M = 10	M = 40	M = 1.4	M = 2	M = 3	M = 5	M = 10	M = 40
-2	-0.08907	0.03785	0.09425	0.08660	0.07616	0.07278	-0.43497	-0.12291	0.12198	0.20607	0.19967	0.19548
-1	-0.18752	-0.05832	0.01949	0.03530	0.02885	0.02726	-0.57272	-0.28452	-0.03932	0.10080	0.11901	0.11778
-0.5	-0.24246	-0.11341	-0.02624	0.00082	-0.00116	-0.00203	-0.64925	-0.37618	-0.13440	0.02407	0.06848	0.06969
0.0	-0.30305	-0.17573	-0.08134	-0.04077	-0.03946	-0.04810	-0.73312	-0.47828	-0.24124	-0.07681	0.00236	0.01003
0.5	-0.37197	-0.24902	-0.15085	-0.10024	-0.09414	-0.10108	-0.82780	-0.59743	-0.36502	-0.20039	-0.10065	-0.07373

second overtone							third overtone					
$\alpha$	M = 1.4	M = 2	M = 3	M = 5	M = 10	M = 40	M = 1.4	M = 2	M = 3	M = 5	M = 10	M = 40
-2	-0.57036	-0.18591	0.11156	0.22028	0.20230	0.19517	-0.65336	-0.23439	0.07975	0.25616	0.25394	0.24798
-1	-0.71485	-0.36758	-0.08123	0.08682	0.10571	0.10248	-0.80728	-0.41541	-0.12031	0.09856	0.15890	0.15543
-0.5	-0.79526	-0.46820	-0.18847	-0.01425	0.04151	0.04193	-0.89457	-0.51186	-0.22976	-0.01835	0.09064	0.09064
0.0	-0.88418	-0.57901	-0.30233	-0.13460	-0.04734	-0.03364	-0.99360	-0.61432	-0.34581	-0.15097	-0.02300	-0.00632
0.5	-0.98658	-0.70854	-0.42526	-0.26062	-0.17023	-0.12223	-1.11324	-0.72772	-0.47406	-0.28919	-0.18986	-0.16158

**Table C6.** Eigenfrequencies ( $\delta_i$ ) for several modes and Mach number  $M$ , for  $\gamma = 7/5$ ,  $\beta = 1$ ,  $R = 1$ .

fundamental							first overtone					
$\alpha$	M = 1.4	M = 2	M = 3	M = 5	M = 10	M = 40	M = 1.4	M = 2	M = 3	M = 5	M = 10	M = 40
-2	0.39767	0.34552	0.29282	0.24754	0.21898	0.20952	1.42551	1.13970	0.87852	0.76775	0.70466	0.68182
-1	0.36781	0.33964	0.30142	0.26912	0.24299	0.23295	1.42305	1.14322	0.86075	0.72474	0.67767	0.65645
-0.5	0.33927	0.32565	0.29805	0.27453	0.25310	0.24316	1.41915	1.14098	0.84834	0.68781	0.64858	0.63132
0.0	0.29464	0.29888	0.28562	0.27146	0.25888	0.24996	1.41348	1.13617	0.83129	0.64222	0.59451	0.58847
0.5	0.21712	0.24788	0.25585	0.25089	0.24871	0.24129	1.40631	1.13033	0.80805	0.58709	0.49800	0.50684

second overtone							third overtone					
$\alpha$	M = 1.4	M = 2	M = 3	M = 5	M = 10	M = 40	M = 1.4	M = 2	M = 3	M = 5	M = 10	M = 40
-2	2.51951	2.05299	1.59806	1.38665	1.26776	1.22410	3.61360	2.98051	2.29947	1.94264	1.78333	1.73160
-1	2.52999	2.04442	1.55067	1.27794	1.18072	1.13988	3.62365	2.95808	2.23096	1.78896	1.66263	1.61282
-0.5	2.53537	2.03446	1.51972	1.20427	1.10224	1.06610	3.62743	2.94199	2.18769	1.69702	1.55241	1.51463
0.0	2.54216	2.01994	1.48060	1.12023	0.97544	0.94493	3.63051	2.92293	2.13719	1.59173	1.38004	1.35762
0.5	2.55310	1.99970	1.43197	1.02115	0.79237	0.71582	3.63317	2.90127	2.08102	1.46210	1.12000	1.02439

**Table C7.** Growth rates ( $\delta_r$ ) for several modes and Mach number  $M$ , for  $\gamma = 7/5$ ,  $\beta = 2$ ,  $R = 1$ .

fundamental							first overtone					
$\alpha$	$M = 1.4$	$M = 2$	$M = 3$	$M = 5$	$M = 10$	$M = 40$	$M = 1.4$	$M = 2$	$M = 3$	$M = 5$	$M = 10$	$M = 40$
-2	-0.09916	0.02373	0.06491	0.06548	0.06276	0.06168	-0.38508	-0.02766	0.18108	0.20098	0.19312	0.18986
-1	-0.18016	-0.04894	0.01531	0.02769	0.02924	0.02951	-0.50806	-0.16818	0.07156	0.13468	0.13438	0.13306
-0.5	-0.22339	-0.08837	-0.01312	0.00598	0.00976	0.01074	-0.57519	-0.24699	0.00248	0.09458	0.10022	0.09991
0.0	-0.26895	-0.13126	-0.04541	-0.01860	-0.01207	-0.01087	-0.64711	-0.33298	-0.07822	0.04517	0.06099	0.06204
0.5	-0.31737	-0.17851	-0.08314	-0.04725	-0.03923	-0.03683	-0.72508	-0.42798	-0.17185	-0.02097	0.01409	0.01680
1	-0.36942	-0.23137	-0.12855	-0.08227	-0.07193	-0.07000	-0.81113	-0.53542	-0.28032	-0.11287	-0.04652	-0.04034

second overtone							third overtone					
$\alpha$	$M = 1.4$	$M = 2$	$M = 3$	$M = 5$	$M = 10$	$M = 40$	$M = 1.4$	$M = 2$	$M = 3$	$M = 5$	$M = 10$	$M = 40$
-2	-0.49741	-0.06810	0.21104	0.23521	0.25707	0.21305	-0.56359	-0.10633	0.20681	0.26949	0.25707	0.25199
-1	-0.62945	-0.22816	0.06747	0.16031	0.15319	0.14976	-0.70059	-0.27195	0.04338	0.19044	0.19003	0.18698
-0.5	-0.70123	-0.31545	-0.01952	0.11185	0.11368	0.11162	-0.77478	-0.36048	-0.05184	0.13461	0.14948	0.14757
0.0	-0.77819	-0.40846	-0.11586	0.04696	0.06709	0.06662	-0.85423	-0.45317	-0.15507	0.05470	0.10113	0.10060
0.5	-0.86211	-0.50851	-0.22079	-0.04384	0.00933	0.01158	-0.94096	-0.55079	-0.26576	-0.05446	0.03875	0.04128
1	-0.95617	-0.61851	-0.33392	-0.16012	-0.07132	-0.05891	-1.03869	-0.65535	-0.38419	-0.18354	-0.05996	-0.04195

**Table C8.** Eigenfrequencies ( $\delta_i$ ) for several modes and Mach number  $M$ , for  $\gamma = 7/5$ ,  $\beta = 2$ ,  $R = 1$ .

fundamental							first overtone					
$\alpha$	$M = 1.4$	$M = 2$	$M = 3$	$M = 5$	$M = 10$	$M = 40$	$M = 1.4$	$M = 2$	$M = 3$	$M = 5$	$M = 10$	$M = 40$
-2	0.38868	0.33930	0.27263	0.21689	0.19035	0.18196	1.38127	1.13340	0.93707	0.80891	0.73527	0.71091
-1	0.35902	0.33269	0.28334	0.23446	0.20783	0.19917	1.38221	1.13281	0.90820	0.79096	0.72107	0.69689
-0.5	0.33488	0.32298	0.28461	0.24175	0.21574	0.20699	1.38113	1.13056	0.89052	0.77352	0.70869	0.68488
0.0	0.30130	0.30690	0.28163	0.24715	0.22278	0.21404	1.37917	1.12659	0.87115	0.74621	0.68991	0.66708
0.5	0.25282	0.28137	0.27222	0.24886	0.22812	0.21960	1.37669	1.12070	0.84953	0.70567	0.65948	0.63946
1	1.37445	0.24006	0.25237	0.24267	0.24167	0.22154	1.37445	1.11318	0.82415	0.65148	0.60833	0.59304

second overtone							third overtone					
$\alpha$	$M = 1.4$	$M = 2$	$M = 3$	$M = 5$	$M = 10$	$M = 40$	$M = 1.4$	$M = 2$	$M = 3$	$M = 5$	$M = 10$	$M = 40$
-2	2.46788	2.05596	1.67481	1.45322	1.87992	1.27679	3.56022	2.99823	2.39725	2.06346	1.87992	1.81889
-1	2.47827	2.05076	1.61887	1.39932	1.27523	1.23173	3.57059	2.98584	2.32761	1.97748	1.80883	1.74957
-0.5	2.48253	2.04491	1.59041	1.35585	1.24071	1.19803	3.57401	2.97612	2.29160	1.91044	1.75631	1.69876
0.0	2.48646	2.03602	1.56062	1.29611	1.19223	1.15126	3.57607	2.96367	2.25222	1.82457	1.68361	1.62958
0.5	2.49055	2.02339	1.52723	1.22149	1.11908	1.08221	3.57653	2.94851	2.20692	1.72610	1.57527	1.53001
1	2.49589	2.00618	1.48773	1.13631	0.99976	0.97002	3.57490	2.93105	2.15397	1.61491	1.40414	1.37197



**Table C9.** Growth rates ( $\delta_r$ ) for several modes and Mach number  $M$ , for  $\gamma = 10/7$ ,  $\beta = 1$ ,  $R = 1$ .

fundamental							first overtone					
$\alpha$	M = 1.4	M = 2	M = 3	M = 5	M = 10	M = 40	M = 1.4	M = 2	M = 3	M = 5	M = 10	M = 40
-2	-0.06194	0.06121	0.11186	0.10098	0.08948	0.08577	-0.39813	-0.08906	0.14898	0.22356	0.21610	0.21184
-1	-0.16697	-0.04057	0.03250	0.04351	0.03815	0.03632	-0.54360	-0.25787	-0.01852	0.11383	0.12907	0.12777
-0.5	-0.22552	-0.09868	-0.01555	0.00856	0.00596	0.00489	-0.62430	-0.35359	-0.11778	0.03503	0.07514	0.07619
0.0	-0.29004	-0.16437	-0.07341	-0.03552	-0.03524	-0.03652	-0.71257	-0.45997	-0.22948	-0.06953	0.00551	0.01260
0.5	-0.36342	-0.24157	-0.14650	-0.09834	-0.09377	-0.10135	-0.81198	-0.58348	-0.35841	-0.19886	-0.10124	-0.07465

second overtone							third overtone					
$\alpha$	M = 1.4	M = 2	M = 3	M = 5	M = 10	M = 40	M = 1.4	M = 2	M = 3	M = 5	M = 10	M = 40
-2	-0.53399	-0.14987	0.14366	0.24185	0.22250	0.21512	-0.61674	-0.19844	0.11267	0.27668	0.27213	0.26647
-1	-0.68645	-0.34045	-0.05850	0.10478	0.11906	0.11547	-0.77867	-0.38962	-0.09781	0.11756	0.17143	0.16835
-0.5	-0.77103	-0.44588	-0.17160	0.02013	0.05088	0.05054	-0.87006	-0.49143	-0.21328	-0.03727	0.10069	0.10093
0.0	-0.86429	-0.56160	-0.29177	-0.12680	-0.04242	-0.03092	-0.97329	-0.59933	-0.33544	-0.14344	-0.01504	0.00141
0.5	-0.97137	-0.69614	-0.42097	-0.26063	-0.17292	-0.12842	-1.09728	-0.71833	-0.46941	-0.28949	-0.19204	-0.16425

**Table C10.** Eigenfrequencies ( $\delta_i$ ) for several modes and Mach number  $M$ , for  $\gamma = 10/7$ ,  $\beta = 1$ ,  $R = 1$ .

fundamental							first overtone					
$\alpha$	M = 1.4	M = 2	M = 3	M = 5	M = 10	M = 40	M = 1.4	M = 2	M = 3	M = 5	M = 10	M = 40
-2	0.41642	0.35499	0.29967	0.25395	0.22603	0.21684	1.44303	1.15321	0.90101	0.79515	0.73329	0.71121
-1	0.39227	0.35418	0.31234	0.27901	0.25313	0.24332	1.44112	1.15748	0.88180	0.75349	0.70664	0.68589
-0.5	0.36680	0.34254	0.31064	0.28603	0.26464	0.25492	1.43701	1.15503	0.86817	0.71530	0.67711	0.65994
0.0	0.32614	0.31826	0.29969	0.28448	0.27185	0.26320	1.43075	1.14950	0.84948	0.66645	0.62159	0.61500
0.5	0.25658	0.27069	0.27121	0.26478	0.26304	0.25612	1.42256	1.14238	0.82394	0.60648	0.51977	0.52818

second overtone							third overtone					
$\alpha$	M = 1.4	M = 2	M = 3	M = 5	M = 10	M = 40	M = 1.4	M = 2	M = 3	M = 5	M = 10	M = 40
-2	2.54187	2.07340	1.63434	1.43693	1.32192	1.28005	3.64394	3.00948	2.34970	2.01372	1.86213	1.80716
-1	2.55276	2.06487	1.58300	1.32636	1.23351	1.19411	3.65474	2.98554	2.27534	1.85363	1.73237	1.68383
-0.5	2.55805	2.05440	1.54974	1.24807	1.15338	1.11841	3.65869	2.96799	2.22839	1.75457	1.61888	1.58174
0.0	2.56455	2.03900	1.50757	1.15783	1.02221	0.99342	3.66181	2.94703	2.17320	1.64157	1.43994	1.42005
0.5	2.57503	2.01765	1.45486	1.05085	0.82754	0.75473	3.66441	2.92314	2.11130	1.50253	1.17500	1.07869

**Table C11.** Growth rates ( $\delta_r$ ) for several modes and Mach number  $M$ , for  $\gamma = 10/7$ ,  $\beta = 2$ ,  $R = 1$ .

fundamental							first overtone					
$\alpha$	$M = 1.4$	$M = 2$	$M = 3$	$M = 5$	$M = 10$	$M = 40$	$M = 1.4$	$M = 2$	$M = 3$	$M = 5$	$M = 10$	$M = 40$
-2	-0.07375	0.04142	0.07763	0.07614	0.07280	0.07155	-0.34620	0.08304	0.20306	0.21684	0.20862	0.20533
-1	-0.16013	-0.03363	0.02499	0.03545	0.03653	0.03665	-0.47564	-0.13749	0.09213	0.14628	0.14536	0.14402
-0.5	-0.20616	-0.07494	-0.00486	0.01226	0.01562	0.01647	-0.54633	-0.21941	0.02188	0.10428	0.10882	0.10856
0.0	-0.25462	-0.11983	-0.03857	-0.01390	-0.00827	-0.00666	-0.62207	-0.30888	-0.06088	0.05333	0.06702	0.06801
0.5	-0.30608	-0.16928	-0.07785	-0.04429	-0.04094	-0.03431	-0.70415	-0.40776	-0.15772	-0.01409	0.01724	0.01981
1	-0.36136	-0.22459	-0.12507	-0.08124	-0.07177	-0.06952	-0.79474	-0.51946	0.27057	-0.10839	-0.04660	-0.04088

second overtone							third overtone					
$\alpha$	$M = 1.4$	$M = 2$	$M = 3$	$M = 5$	$M = 10$	$M = 40$	$M = 1.4$	$M = 2$	$M = 3$	$M = 5$	$M = 10$	$M = 40$
-2	-0.45725	-0.02799	0.23935	0.25393	0.23740	0.23158	-0.52277	-0.06505	0.23978	0.28767	0.27496	0.26999
-1	-0.59644	-0.19541	0.09387	0.17485	0.16706	0.16359	-0.66723	-0.23918	0.07249	0.20509	0.20327	0.20036
-0.5	-0.67202	-0.28688	0.00398	0.12490	0.12502	0.12288	-0.74529	-0.33252	-0.02677	0.14883	0.16022	0.15847
0.0	-0.75293	-0.38439	-0.09660	0.05923	0.07562	0.07504	-0.82866	-0.43035	-0.13511	0.06892	0.10918	0.10883
0.5	-0.84094	-0.48922	-0.20689	-0.03333	0.01469	0.01648	-0.91932	-0.53338	-0.25170	-0.04312	0.04414	0.04659
1	-0.93927	-0.60418	-0.32616	-0.15479	-0.06935	-0.05869	-1.02094	-0.64359	-0.37639	-0.17891	-0.05673	-0.03993

**Table C12.** Eigenfrequencies ( $\delta_i$ ) for several modes and Mach number  $M$ , for  $\gamma = 10/7$ ,  $\beta = 2$ ,  $R = 1$ .

fundamental							first overtone					
$\alpha$	$M = 1.4$	$M = 2$	$M = 3$	$M = 5$	$M = 10$	$M = 40$	$M = 1.4$	$M = 2$	$M = 3$	$M = 5$	$M = 10$	$M = 40$
-2	0.40777	0.34899	0.27836	0.22238	0.19627	0.18805	1.39652	1.14917	0.96382	0.83731	0.76595	0.74242
-1	0.38242	0.34567	0.29182	0.24202	0.21576	0.20728	1.39809	1.14834	0.93484	0.82038	0.75204	0.72862
-0.5	0.36056	0.33752	0.29438	0.25021	0.22449	0.21592	1.39700	1.14576	0.91599	0.80349	0.73960	0.71648
0.0	0.32969	0.32302	0.29263	0.25649	0.23227	0.22371	1.39478	1.14127	0.89488	0.77648	0.72056	0.69829
0.5	0.28523	0.29923	0.28435	0.25909	0.24375	0.22994	1.39174	1.13455	0.87115	0.73511	0.68958	0.66984
1	0.21596	0.26026	0.26545	0.25378	0.24375	0.23248	1.38863	1.12577	0.84331	0.67783	0.63389	0.62167

second overtone							third overtone					
$\alpha$	$M = 1.4$	$M = 2$	$M = 3$	$M = 5$	$M = 10$	$M = 40$	$M = 1.4$	$M = 2$	$M = 3$	$M = 5$	$M = 10$	$M = 40$
-2	2.48776	2.07883	1.72004	1.50427	1.37695	1.33440	3.58806	3.02976	2.45907	2.13679	1.95887	1.89990
-1	2.49901	2.07324	1.65964	1.45075	1.33032	1.28845	3.59971	3.01646	2.38219	2.05082	1.88589	1.82855
-0.5	2.50345	2.06711	1.62817	1.40732	1.29510	1.25394	3.60359	3.00599	2.34254	1.97917	1.83180	1.77601
0.0	2.50732	2.05776	1.59542	1.34632	1.24561	1.20599	3.60600	2.99246	2.29962	1.89361	1.75697	1.70439
0.5	2.51109	2.04442	1.55905	1.26750	1.17088	1.13507	3.60672	2.97582	2.25045	1.78809	1.64565	1.60118
1	2.51579	2.02624	1.51615	1.17580	1.04800	1.01950	3.60532	2.95646	2.19278	1.66852	1.46825	1.43775

**Table C13.** Critical values of  $\alpha$  for various modes and Mach number M of different cases for R = 1.

fundamental					first overtone			
$(\beta, \gamma)$	M = 1.4	M = 2	M = 3	M = 5	M = 1.4	M = 2	M = 3	M = 5
(1, 5/3)	-1.029	-0.423	-0.067	0.081	-2.613	-1.280	-0.491	-0.058
(2, 5/3)	-1.031	-0.309	0.134	0.312	-2.330	-0.630	0.246	0.659
(1, 7/5)	-3.009	-1.588	-0.776	-0.488	-6.044	-2.870	-1.222	-0.368
(2, 7/5)	-3.320	-1.673	-0.723	-0.372	-5.898	-2.214	-0.483	0.359
(1, 10/7)	-2.646	-1.380	-0.652	-0.391	-5.421	-2.593	-1.100	-0.317
(2, 10/7)	-2.907	-1.434	-0.577	-0.257	-5.255	-1.939	-0.359	0.409

second overtone					third overtone			
$(\beta, \gamma)$	M = 1.4	M = 2	M = 3	M = 5	M = 1.4	M = 2	M = 3	M = 5
(1, 5/3)	-3.312	-1.536	-0.631	-0.160	-3.667	-1.718	-0.760	-0.207
(2, 5/3)	-2.861	-0.828	0.152	0.643	-3.143	-0.984	0.049	0.620
(1, 7/5)	-7.111	-3.159	-1.401	-0.563	-7.609	-3.426	-1.583	-0.573
(2, 7/5)	-6.728	-2.461	-0.607	0.279	-7.136	-2.693	-0.766	0.266
(1, 10/7)	-6.430	-2.878	-1.273	-0.499	-6.908	-3.133	-1.447	-0.514
(2, 10/7)	-6.037	-2.178	-0.479	0.339	-6.426	-2.399	-0.630	0.324

**Table C14.** Critical values of  $\alpha$  for various modes and Mach number M of different cases for R = 0.

fundamental					first overtone			
$(\beta, \gamma)$	M = 1.4	M = 2	M = 3	M = 5	M = 1.4	M = 2	M = 3	M = 5
(1, 5/3)	0.407	0.201	0.106	0.068	-0.106	-0.071	0.047	0.114
(2, 5/3)	0.014	0.002	0.183	0.310	-0.019	0.366	0.604	0.719
(1, 7/5)	0.220	-0.200	-0.413	-0.495	-0.377	-0.336	-0.098	0.022
(2, 7/5)	-0.794	-0.886	-0.585	-0.370	-0.752	-0.078	0.349	0.555
(1, 10/7)	0.248	-0.133	-0.325	-0.399	-0.333	-0.292	-0.076	0.036
(2, 10/7)	-0.660	-0.737	-0.456	-0.256	-0.631	-0.006	0.389	0.579

second overtone					third overtone			
$(\beta, \gamma)$	M = 1.4	M = 2	M = 3	M = 5	M = 1.4	M = 2	M = 3	M = 5
(1, 5/3)	0.063	0.039	0.026	0.025	-0.085	-0.019	0.103	0.142
(2, 5/3)	0.122	0.526	0.688	0.758	0.225	0.572	0.750	0.838
(1, 7/5)	-0.225	-0.195	-0.235	-0.235	-0.328	-0.238	0.008	0.014
(2, 7/5)	-0.439	0.232	0.447	0.534	-0.253	0.274	0.594	0.736
(1, 10/7)	-0.184	-0.161	-0.196	-0.197	-0.291	-0.203	0.023	0.037
(2, 10/7)	-0.347	0.278	0.485	0.569	-0.177	0.321	0.617	0.752